PITTING CORROSION BEHAVIOUR OF ALUMINIUM ALLOYS

LEON MEI CHEN

BACOLEOR ENGINEERING MECHANICAL
UNIVERSITY MALAYSIA PAHANG

PITTING CORROSION BEHAVIOUR OF ALUMINIUM ALLOYS

LEON MEI CHEN

Report submitted in partial fulfilment of the requirements for the award of the degree of
Bachelor of Mechanical Engineering

Faculty of Mechanical Engineering
UNIVERSITI MALAYSIA PAHANG

JUNE 2013

UNIVERSITI MALAYSIA PAHANG
FACULTY OF MECHANICAL ENGINEERING

I certify that the project entitled “Pitting Corrosion Behaviour of Aluminium Alloy” is written by Leon Mei Chen. I have examined the final copy of this project and in my opinion; it is fully adequate in terms language standard, and report formatting requirement for the award of the degree of Bachelor of Engineering. I herewith recommend that it be accepted in partial fulfilment of the requirements for the degree of Bachelor of Mechanical Engineering.

NORHAZIDA BINTI AB.RAZAK

Examiner **Signature**

SUPERVISOR'S DECLARATION

I hereby declare that I have checked this project and in my opinion, this project is satisfactory in terms of scope and quality for the award of the degree of Bachelor of Mechanical Engineering.

\'

Signature : **……**
Name of Supervisor : MADAM NUR AZHANI BINTI ABD RAZAK
Position : LECTURER
Date : **……**

STUDENT'S DECLARATION

I hereby declare that the work in this project is my own except for quotations and summaries which have been duly acknowledged. The project has not been accepted for any degree and is not concurrently submitted for award of other degree.

Signature : **……**
Name : LEON MEI CHEN
ID Number : MA09085
Date : **……**

Specially dedicated to

My beloved family and those who have guided and inspired me

Throughout my journey of learning

ACKNOWLEDGEMENTS

I am grateful and I would like to express my sincere gratitude to my supervisor, Madam Nur Azhani binti Abd Razak for her germinal ideas, invaluable guidance, continuous encouragement and constant support in making this research possible. She has always impressed me with her outstanding professional conduct, her strong conviction for science, and her belief that a Degree of Bachelor program is only a start of a life-long learning experience. I appreciate her consistent support from the first day I applied to graduate program to these concluding moments. I am truly grateful for her progressive vision about my training in science, her tolerance of my naive mistakes, and her commitment to my future career. I also sincerely thanks for the time spent proofreading and correcting my many mistakes.

My sincere thanks go to all my coursemates and members of the staff of the Mechanical Engineering Department, UMP, who helped me in many ways and made my stay at UMP pleasant and unforgettable.

I acknowledge my sincere indebtedness and gratitude to my parents for their love, dream and sacrifice throughout my life. I am also grateful to family members for their sacrifice, patience, and understanding that were inevitable to make this work possible. I cannot find the appropriate words that could properly describe my appreciation for their devotion, support and faith in my ability to attain my goals. Special thanks should be given to my friends. I would like to acknowledge their comments and suggestions, which was crucial for the successful completion of this study.

ABSTRACT

The present work is aimed to investigate the effect of temperature and concentration of solution on the pitting corrosion of AA6061 – T6 aluminium alloy and study its electrochemical behaviour and physical behaviour in sodium chloride (NaCl) solution using the polarization technique. The experiments were carried out under static conditions at different NaCl concentration solutions (3.5, 4.5 and 5.5) wt% and different temperatures (25, 35, 45, 55 and 65) ^{o}C. This experiment started with different NaCl concentration solutions at room temperature condition by using potentiostat/galvometer instrument. Water bath machine had been used to control the solution temperature in this experiment. Natural pitting corrosion experiment had been tested for 2 months in different NaCl concentration solutions. Comparison between two methods which were tested in different concentration was discussed. It was found experimentally that increasing in NaCl concentration and temperatures lead to decrease in the breakdown potential (E_{corr}) and increase in corrosion rate of as-received materials. Based on the results obtained, the corrosion rate increased from 0.1529 mmpy to 0.3650 mmpy for the electrochemical experiment and 0.2517 mmpy to 0.4692 mmpy for natural pitting when concentration of the solutions increased from 3.5 wt% to 5.5 wt%. The influence of solutions' temperature (25 – 65 ^{o}C) on the pitting corrosion of AA6061-T6, showed the changes of the corrosion rate from 0.1529 mmpy to 1.205mmpy. In conclusion, the highest corrosion rate obtained at the highest solution temperature. The increased in concentration and temperature lead to the increasing of corrosion rate of AA6061-T6.

ABSTRAK

Satu eksperimen yang bertujuan mengkaji kesan-kesan beberapa pembolehubah terhadap hakisan bopeng pada AA 6061-T6 aloi aluminium dan mengkaji fizikal elektrokimia dan fizikal dalam larutan batrium kloida (NaCl) dengan menggunakan teknik polarisasi telah dijalankan. Kajian ini telah dijalankan dengan menggunakan pelbagai kepekatan NaCl ((3.5, 4.5, 5.5) wt% dan suhu yang berbeza (25, 35, 45, 55 and 65) ^{o}C. Eksperimen ini bermula dengan larutan yang berbeza kepekatan NaCl pada keadaan suhu bilik. “Water bath” yang boleh mengawal suhu larutan NaCl telah digunakan dalam eksperimen. Terdapat satu eksperimen semulajadi bagi hakisan bopeng telah dikaji dalam dua bulan dengan menggunakan larutan kepekatan NaCl yang berbeza. Perbandingan dua kaedah yang berbeza digunakan untuk menguji kehakisan dalam kepekatan yang berbeza telah dinyatakan. Eksperimen peningkatan dalam kepekatan dan suhu larutan NaCl mengakibatkan penurunan dalam potensi kerosakan (E_{corr}) dan meningkatkan kadar hakisan sampel yang diujikan. Berdasarkan keputusan yang diperolehi, kadar hakisan bagi eksperimen elektrokimia menambah dari 0.1529 mmpy sehingga 0.3650 mmpy. Bagi bopeng semula jadi, kadar hakisan telan meningkat dari 0.2517 mmpy sehingga 0.4692 mmpy semasa kepekatan larutan NaCl meningkat dari 3.5wt% sehingga 5.5wt%. Kadar hakisan menunjukkan perubahan dari 0.1529 mmpy dan meningkat sehingga 1.205 mmpy bagi suhu larutan NaCl yang berbeza (25 – 65) ^{o}C. Kesimpulannya, pada suhu 65^{o}C mendapat kadar hakisan yang paling tinggi. Peningkatan kepekatan dan suhu menyebabkan peningkatan kadar kakisan AA6061-T6.

TABLE OF CONTENTS

LIST OF TABLES

LIST OF FIGURES

LIST OF SYMBOLS

A	Exposed area
d	Density
E	Potential
E_B	Breakdown potential
E_b	Transpassivation potential/ critical pitting potential
E_{corr}	Corrosion potential
E_p	Pitting potential
E_{pp}	Critical passivation potential
E_R	Repassivation potential
$E_{rev,\ O2}$	Reversible potential of the oxygen electrode
i	Current density
I_{corr} / i_c	Corrosion current density
$i_{c,h}$	Final free corrosion current density
i_{pp}	Passivation current density
K	Constant value
r	Pit radius or depth
t	Time
$\%$	Percentage
^oC	Celcius
α	Direct proportional
β_a	Anodic Tafel constant
β_c	Cathodic Tafel conctant

LIST OF ABBREVIATIONS

Al	Aluminium
Al_3^+	Aluminium ion
Al_2O_3	Aluminium Oxide
CPT	Critical pitting temperature
Cl^-	Chloride ion
Cr	Chromium
CR	Corrosion rate
Cu	Copper
e^-	Electron
EW	Equivalent weight
Fe	Iron
H^+	Hydrogen ion
H_2O	Water
i.e.	Id est (means in Latin “that is”)
IR	Infrared radiation
Mn	Manganese
mmpy	Milimeter per year
mpy	Mils per year
M.V.	Mean Value
NaCl	Sodium chloride
O_2	Oxygen
OH^-	Hydroxide irons
pH	Power of Hydrogen

P.P.D.	Pits population density
SCE	Saturated calomel electrode
SEM	Scanning electron microscopy
Si	Silicon
SIC	Silicon carbide
SS	Stainless steel
Ti	Titanium
UMP	University Malaysia Pahang
Wt%	Weight percentage
Zn	Zinc

CHAPTER 1

INTRODUCTION

1.1 INTRODUCTION

This chapter explains about the background of study, problem statement, objectives and the scopes of this study. The main purpose for this study can be identified by referring at the problem statement of this study. Furthermore, the details of this study and outcome can be achieved on the objectives and its scopes.

1.2 BACKGROUND OF STUDY

Corrosion can be defined as degradation of a material's properties because of chemical reaction between the components of the material with their environments (Shaw and Kelly, 2006). Appearance of corrosion not only created variety of problems for daily life, but it also has a huge economic and environmental impact on virtually all facets of the world's infrastructure, from highways, bridges, and buildings to oil and gas, chemical processing, and water and wastewater systems (Günter, 2009).

The Electrochemical Society Interface states that aluminium alloys are the largest proportions of nonferrous alloys that are widely used in industrial applications, especially for construction and equipment, containers and packaging, production of automotive, aviation, aerospace, household appliances electronics, food industry, and majority of commercial marine applications. Aluminium and its alloys are characterized by a relatively good electrical and thermal conductivities, low density (2.71 g/cm^3), high ductility and high corrosion resistance. There have several parameters affect the behaviour of aluminium alloys in aqueous environments. The surface properties of the material, nature environment effect, surrounding temperature, pH and the composition

of the aggressive solution influences the composition and microstructure of aluminium alloys. Moreover, mechanical and heat treatment processes also affect the structure and composition of oxide layer on the material surface, which cause more corrosion resistant.

Due to light weight and excellent machining properties, many ship superstructures and liquid cargo containers are made by aluminium alloys. The 5000 series and 6000 series alloys which demonstrate adequate strength and excellent corrosion resistance are the most popular aluminium alloys for use in corrosive environments such as seawater. AA6061-T6 aluminium alloyed with magnesium and silicon displays high strength, excellent extrudability, reasonable weldability and good corrosion resistance. This alloy finds widespread application in ship building (civil and military) and in the fabrication of tank containers for transporting various liquids, where is often welded during manufacturing process. However, this material tends to corrode in chloride-containing environments and form in pitting corrosion.

The aluminium-rich matrix adjacent to magnesium-silicon intermetallic precipitates or silicon-rich phases in aluminium-silicon-magnesium alloys has been shown to be susceptible to preferential corrosion in NaCl solutions. Coarse intermetallic particles containing aluminium, silicon and magnesium act as nucleation sites for pit formation. The formation of pits, in turn, has a detrimental effect on the fatigue life of 6061 aluminium. The fatigue life of aluminium alloys has been shown to be significantly reduced when tested in a 3.5% NaCl solution compared to the fatigue life of the same alloy in air. This reduction in fatigue life has been attributed to premature crack initiation from surface pits by and higher crack growth rate resulting from synergistic interaction of fatigue and stress corrosion. Although the pitting corrosion behaviour of AA6061 has been studied in depth, its behaviour when simultaneously subjected to a corrosive environment consisting of simulated sea water (or a 3.5% NaCl solution) is not well understood. This investigation studied the corrosion behaviour of aluminium 6061 in the T6 temper condition, and determined the corrosion damage due to influence of temperature and concentration of solution (Kalenda, 2011).

1.3 PROBLEM STATEMENT

Pitting corrosion always influences the local strength of ship hull members. Water pollution and global warming problem affect the concentration of chloride and temperature of seawater increase. When concentration of chloride in seawater increases, it directly increase corrosion rate to the marine applications. Formation of passive films on deterioration aluminium alloys is because of the presence of dissolved oxygen, and chloride ion. This will reduce life time of the product and increase liability marine product. Marine application corrodes rapidly when the temperature of seawater increases. The diffusion of chloride ion through the passive film increases at higher seawater's temperature. Therefore, research of pitting corrosion behaviour in aluminium alloy because of temperature and concentration of seawater are highly beneficial for its prevention in future.

1.4 OBJECTIVES

The main objective of this study is to investigate the pitting corrosion behaviour of aluminium alloy in different concentrations of chloride solution and under static conditions at different temperatures.

1.5 SCOPE

The scopes of this project are as follows:

i. The material that used in this project is AA6061-T6 aluminium alloy.
ii. Different temperatures (25 ℃, 35 ℃, 45 ℃, 55 ℃, 65 ℃) and chloride concentrations (3.5, 4.5 and 5.5 wt%) are used in this study.
iii. Microstructure analysis of the specimens by using scanning electron microscope (SEM).
iv. Electrochemical test is performed by using potentiostat/ galvometer instrument.
v. Corrosion rate is analyzed by IV Man software.

1.6 THESIS OUTLINE

This thesis consists of 5 chapters which illustrate the flow work of this project from introduction until end of the conclusion. There are different contents present in each chapter. Reader will be more understand the detail of the project and obtains the output of the project after they read the entire chapters in thesis.

Chapter 1 discusses the background of the study, problem statement, objectives, and the scope of this study.

Chapter 2 contains all the literature reviews of this study. This chapter also discusses some detail of material that used in this study (aluminium alloy). Detail of pitting corrosion is discussed in Chapter 2. Some explanation of microstructure analysis also will be explained in this chapter.

Chapter 3 discusses the summary of the research methodology of this project. The progress of this project is explained.

Chapter 4 contains the results that achieved during the experiment in this study. This chapter also explains the analysis and discussion of the results of experiment.

Chapter 5 discusses the conclusions of the project. This chapter also contains some future recommendation of this study.

CHAPTER 2

LITERATURE REVIEW

2.1 INTRODUCTION

This chapter discusses about phenomena of pitting corrosion, material that used in this project – aluminium alloys and parameters of pitting corrosion that react on aluminium alloys. The first topic explains about the mechanism of pitting corrosion. Stages of pitting corrosion will be explained in detail. Based on the chemical reaction, the formation of pitting corrosion on aluminium alloys in seawater is explained. AA6061 aluminium alloys that are used in this study which include its properties and some explanation about the chosen material are presented. Pitting on AA6061-T6 aluminium alloys is influenced by many different parameters, including concentration of seawater and temperature. Explanation of each parameter will be discussed in this chapter.

2.2 PITTING CORROSION

Pitting corrosion is an electrochemical oxidation-reduction (redox) process which occurs within localized holes on the surface of metal coated with a passive film. Many engineering alloys, such as aluminium alloy are useful because passive film, which are tin oxide layers that in neutral, weakly acidic or alkaline aqueous media on the metal surface greatly reduce the rate of corrosion of the alloys (Frankel, 1998). Accelerated dissolution of the underlying metal occurs because passive film susceptible to localized breakdown. Potential, pH and the duration immerse in aqueous environment are the influences that affect the thickness and structure of oxide film (Naseer et.al, 2007). Figure 2.1 shows the microphotograph of piting corrosion on a un-clad 2024 aluminium alloy.

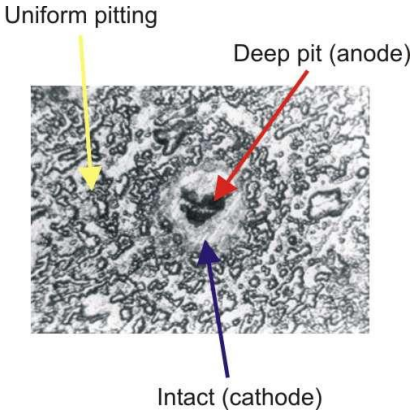

Figure 2.1: Microphotograph of piting corrosion on a un-clad AA2024 aluminium alloy

Source: World's Premier Independent Aviation News Resource

Pitting corrosion is caused by several species such as chloride ions are present in the electrolyte solutions. Normally a pit will occur as a cavity or hole with the surface diameter about some as or less than the depth. Most of the pits develop and grow downward and horizontal surfaces. There are varies of number and shapes in pitting corrosion. Figure 2.2 shows seven typical pit shapes: narrow and deep pits exhibiting crystalline attack, elliptical pit, wide and shallow pits with a polished surface, subsurface/occluded pits growing under a cover constituted of corrosion product or non-corroded metal, undercutting pit, horizontal pit and vertical pit (Ma, 2012).

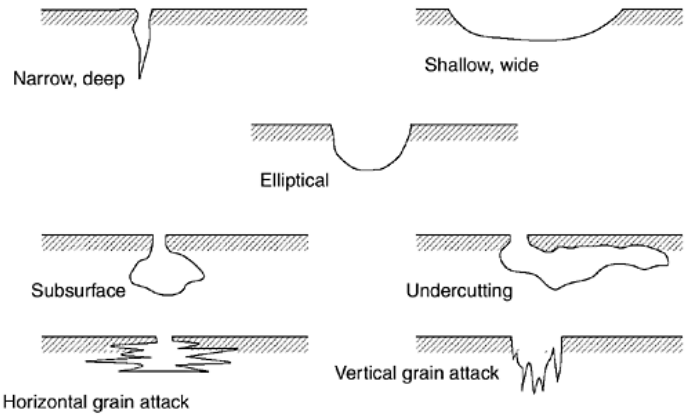

Figure 2.2: Typical pit shapes

Source: Web Corrosion Services

Pitting corrosion is associated with active-passive type alloys and occurs under condition specific to each alloy and environment. Corrosion of pit is a unique type of anodic reaction which is an autocatalytic process in nature. Once a pit starts to grow, the corrosion processes within a pit produce conditions which are both stimulating and necessary for the continuing activity of the pit. This is illustrated schematically in Figure 2.3. The metal is being pitted by an aerated Sodium Chloride (NaCl) solution. The rapid dissolution of metal within the pit tends to produce an excess of positive charge in this area resulting in the migration of chloride ions to maintain electroneutrality, while the oxygen reduction takes place on the adjacent metal surfaces.

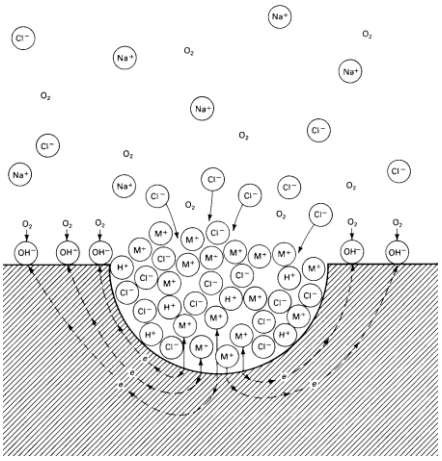

Figure 2.3: Autocatalytic process occurring in a corrosion pit.

Source: U.R.Evans, Corrosion, 7:238 (1951)

Presence of aggressive anion species and chloride ions will affect the formation of passive film breakdown of pitting corrosion (Leckie and Uhlig, 1996). The severity of pitting tends to vary with the logarithm of the bulk chloride concentration. The reason for the aggressiveness of chloride has been pondered for some time, and a number of notions have been put forth.

Consequently, the term concentration cell corrosion has been used to describe the base pitting corrosion. To illustrate the basic mechanism of pitting corrosion, consider a riveted plate section of aluminium alloy immersed in aerated seawater as shown in

Figure 2.3. The overall reaction involves the dissolution of aluminium and the reduction of oxygen to hydroxide ions.

Oxidation: $Al \rightarrow Al^{3+} + 3e^-$ Equation 2.1

Reduction: $O_2 + H_2O + 4e \rightarrow 4OH^-$ Equation 2.2

An oxidation or anodic reaction is indicated by an increase in valence of electron. The local pit environment becomes depletes in cathodic reactant (eg.oxygen), shifts most of the cathodic reaction (such as given by equation 2.1) to boldly exposed surface outside of the pit cavity where this reaction is more plentiful. The pit environment becomes more corrode in metal cations as a result of the dissolution process in the pit grows (Equation 2.3). The concentration of an anodic species such as chloride must increase within the pit in order to maintain charge neutrality by balancing the charge associated with the cation concentration. The positively charged pit attracts negative ions of chlorine Cl^- increasing acidity of the electrolyte according to the reaction:

Overall: $Al^{3+} + 3H_2O \rightarrow Al_2O_3 + 6H^+$ Equation 2.3

The pH in the pit is lower (acidity increases) causes acceleration of corrosion process.

As concludion, the local pit environment is reduced in cathodic reactant, such as dissolved oxygen, enriched in metal cation and anionic species (chloride) and acidified. The acidic chloride environment thus generated in pits is aggressive to most metals and tends to propagate the pit growth.

Current density within the pit used to measure the pit penetration rate. The ionic concentration in the pit solution increases when the pit density increases, often reaching supersaturation conditions. Under the alternating current, pitting in aluminium dissolution takes place during the anodic half period, while reduction of protons during the cathodic half period. This will rise in the pH, provoke the formation of a passivating film, resulting in the redistribution of attack. It was obvious from the micrographs (Figure 2.4) that the increase of the current density influenced the graining morphology in the number and the size of the pits. It was also observed by the respective histograms from the image analysis that as the current density increases, the pits population density

(P.P.D.) decreased, while the mean value (M.V.) of the pits size increased (Figure 2.5) (Dimogerontakisa et.al.).

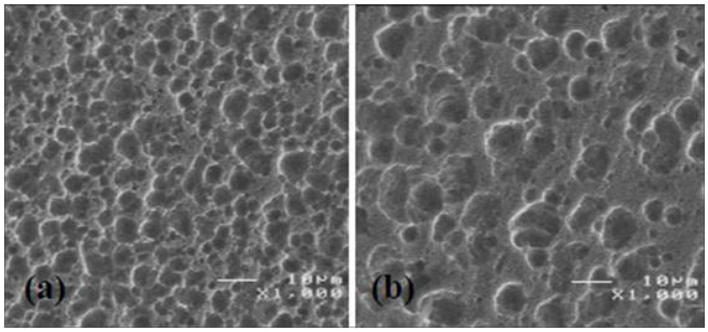

Figure 2.4: SEM micrographs (x1.000) of samples grained with 960 C dm^{-2} at (a) 40 A dm^{-2} and (b) 120 A $dm^{-2.}$

Source: Dimogerontakisa , Campestrinib and Terryna (2006)

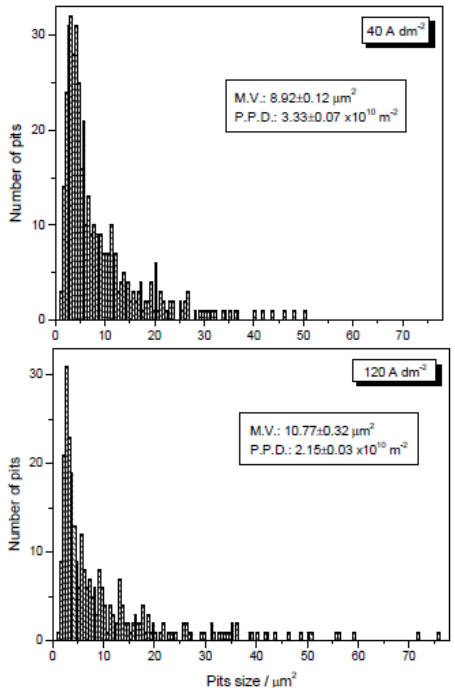

Figure 2.5: Distribution of the pits size for AC-graining with 480 C dm^{-2} at 40 and 120A dm^{-2}

Source: Dimogerontakisa , Campestrinib and Terryna (2006)

2.2.1 Stages of Pitting

Szklarska-Smialowska (1998) states the following four stages of the pitting corrosion process:

i. Process occurring on the passive film;
ii. Process occuring within the passive film, when no visible changes occur in the film;
iii. Formation of so-called metastables pits which initiate and grow below critical pitting potential and then repassivate;
iv. Stable pit growth, above a critical pitting potential.

The initiation and growth of corrosion pit has been, for the purpose of this sub-chapter, divided in 4 steps described (Figure 2.6). Specific examples of pit morphologies representative of the schematic in Figure 2.6 are shown in Figure 2.7.

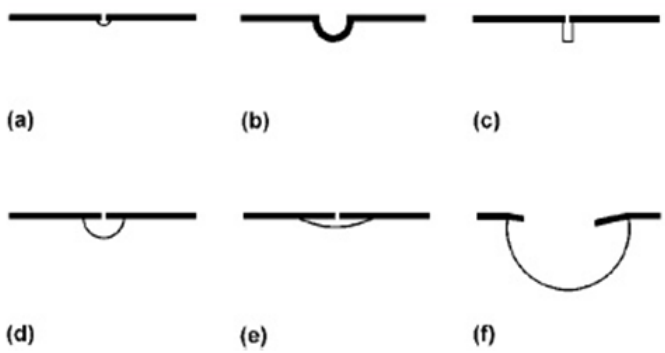

Figure 2.6: Schematic representation of shapes of pit initiation and propagation
Source: Fundamentals of Electrochemical Corrosion

Source: Hewette (1978)

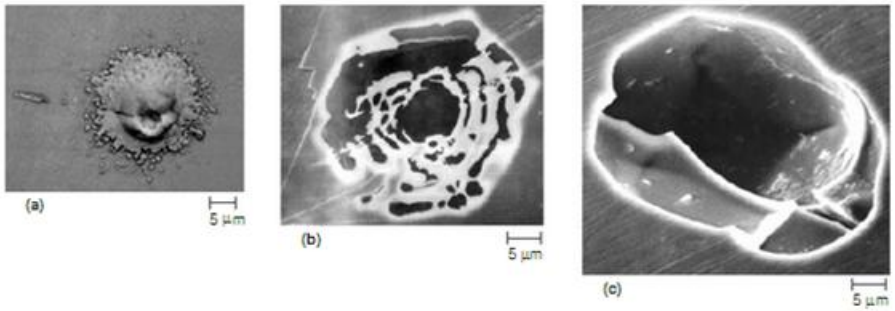

Figure 2.7: Stage of penetration of passive film leading to corrosion pit formation. (a) Initial stage of pit formation. (b) Partially perforated passive film on pit. (c) Fragment of passive film on edge pit.

Source: Hewette (1978)

2.2.1.1 Pit Initiation and Passive Film Breakdown

Breakdown is an occurrence that happens rapidly on a very small scale, making direct observation difficult (Frankel, 1998). Pit initiation and passive film breakdown can be categorized in three type mechanisms which is focus in passive film penetration, film breaking or adsorption (Figure 2.8). The passive film changes in a range of composition, structure, thickness and protectiveness depend on alloy composition, potential, environment, and exposure history (Frankel, 1998). Passive layer form on the reactive metals will increase until 100V without existing of oxygen evolution with thickness reaching several tens of nanometers in thickness to the potential for oxygen evolution. However, the existence of semiconducting properties, valve metals can grow up to a few nanometers in thickness to the potential for oxygen evolution. Figure 2.8 (a) shows the penetration mechanisms for pit initiation where a potential drop at the metal oxide and the oxide-electrolyte interface in these films as well as within the passive layer (Strehblow and Marcus, 1995). In order to initiate pitting corrosion, the aggressive ions migrate into the passive film with penetration method and take place to bring the metal in contact with the aggressive ions solution (Figure 2.8 (b). The adsorption mechanism starts with migration of aggressive anion which is simulated by high electric field in the film. Pitting starts to react when high current circulate through the contaminated zone (Alvarez and Galvele, 2010). Pitting initiation by a film breaking

mechanism can consider that the thin passive film is in continual state of breakdown and repair. In the Figure 2.8 (c) on the basic of adsorption theories of ignition were first based on the nation of competitive adsorption of chloride ions and oxygen. Chloride migrates to the oxide interface and forms a metal chloride phase that can crack the overlaying oxide as a result of its larger specific volume.

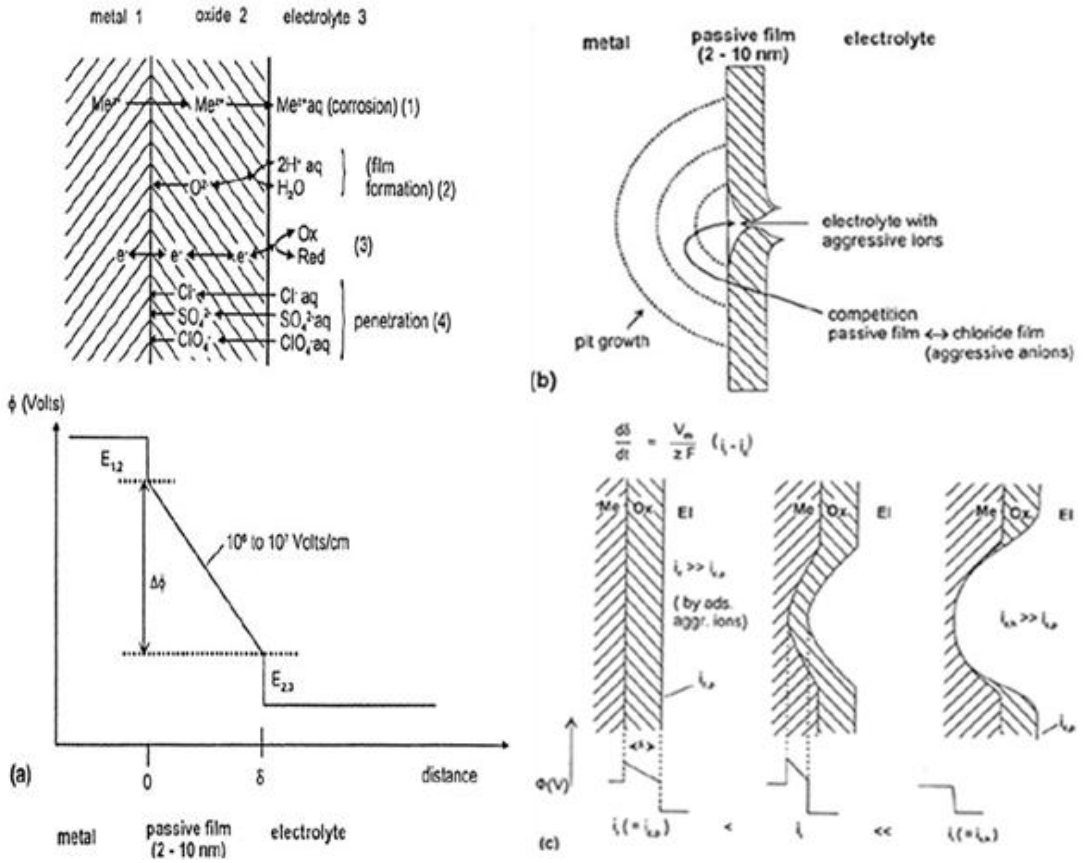

Figure 2.8: Phase diagram of a passive metal demonstrating the processes leading to pit nucleation. (a) Penetration mechanism and phase diagram of a passive layer with related processes of ion and electron transfer within the oxide and at its phase boundaries including schematic potential diagram (Φ). (b) Film breaking mechanism and related competing processes. (c) Adsorption mechanism with increased local transfer of metal ions and related corrosion current density, i_c caused by complex aggressive anions leading to thinning of the passive layer and increases layer field strength and final free corrosion current density $i_{c,h}$ within the pit.

Source: Strehblow (1976)

2.2.1.2 Metastable Pitting

Metastable pits are pits that grow for a limited period before repassivating (Frankel, 1998). Matastable pit growth is a characteristic feature of the pitting corrosion of aluminium alloys which are covered by a layer that is a survival of the passive film, and then undergoes a rupture process and repassivation of the pits (Alvarez and Galvele, 2010). Metastable pit growth in micron size with a life time on the order of seconds (Rao et.al., 2004) at potentials far below the pitting potential and also above the pitting potential during the induction time prior to the onset of stable pitting (Frankel, 1998). Pit stability depends on the pit size, the duration of time lapse at the open circuit the potential and upon applied potential (Szklarska-Smialowska, 1998). Typical metastable pit current transients on stainless steels show on Figure 2.9, which solutes in chloride solution under an applied anodic potential. The growth of metastble pit is depended to pit current. After a short growth period, the sharp current quickly decreases back to level of the original passive current due to repassivation process of metastable pits. The porous cover ruptures and the pit electrolyte dilutes can cause the metastable pits repassivate (Rao et.al., 2004).

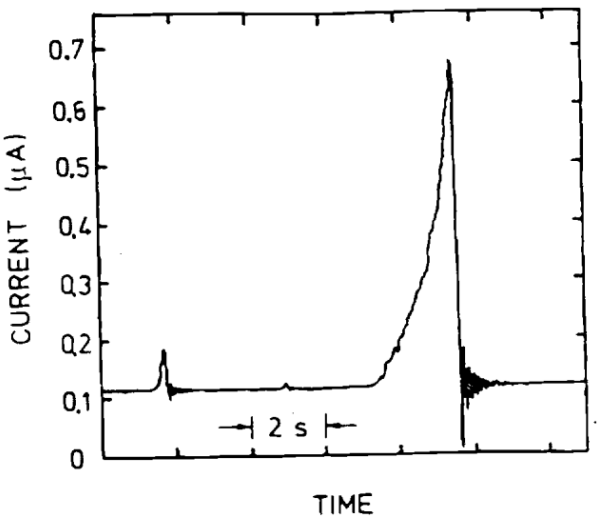

Figure 2.9: Typical metastable pit transients observed on 302 stainless steel polarized at 420mV SCE in 0.1M NaCl solution.

Source: Frankel (1998)

2.2.1.3 Stable Pitting and Pit Growth

Rate of pit growth and pit stability are depended upon the maintenance of pit electrolyte composition and pit bottom potential that are at least severe enough to prevent repassivation of the dissolving metal surface at the pit bottom. Pit growth kinetics influenced by the mass-transport characteristics of the pit through the pit electrolyte concentration.

Pit growth can be controlled by some factors that can limit any electrochemical reaction, such as charge-transfer processes (activiation), mass transport, ohmic effect, or some combination of these factors. For a hemispherical pit, different of rate controlling factors will lead to specific relationships between current *I*, current density *i*, pit radius or depth *r*, time *t*, and potential *E*.

Under charge transfer control, Tafel's law describes $I \alpha exp\ E$.
Under ohmic control, it can be derived $I \alpha r$ and $I \alpha \frac{I}{r^2}\ \alpha \frac{I}{r}$. From Faraday's law, $i \alpha \frac{dr}{dt}$, leading to $r \alpha t^{\frac{1}{2}}$ and thus $I \alpha t^{\frac{1}{2}}$ and $I \alpha t^{\frac{1}{2}}$. Ohm's law determine I α E.
Under mass transport control, according to Fick's laws, $I \alpha \frac{I}{r}$, thus $i \alpha t^{-\frac{1}{2}}$, I is E independent.

The current measures from a sample held at a fixed potential may come from several pits with unknown active pit surface area (Alvarez and Galvele, 2010). Pit growth at low potentials below the range of limiting pit current densities is controlled by a combination of ohmic, charge transfer, and concentration over potential factors. At high potentials, mass transport may be rate controlling. Mass transport determines the stability of pits even at lower potentials, because the local environment controls passivation. The rate of pit growth decreases with time for pitting controlled by either ohmic or mass-transport effects. The pit growth rate often varies with t^{-n}, where *n* is approximately equal to 0.5.

There are three limitations on the dissolution rate at pitting site shows in Figure 2.10. Figure 2.10 (a) shows that diffusional effect at the cathode (increases in the

boundary layer thickness with time limits the cathodic current). Salt film precipitation at anode i.e exceeding the solubility of the metal salts causes a porous film to form across which some of the driving force drops (Figure 2.10 (b)). Ohmic effects in the solution in the solution between anode and cathode show in Figure 2.10 (c).

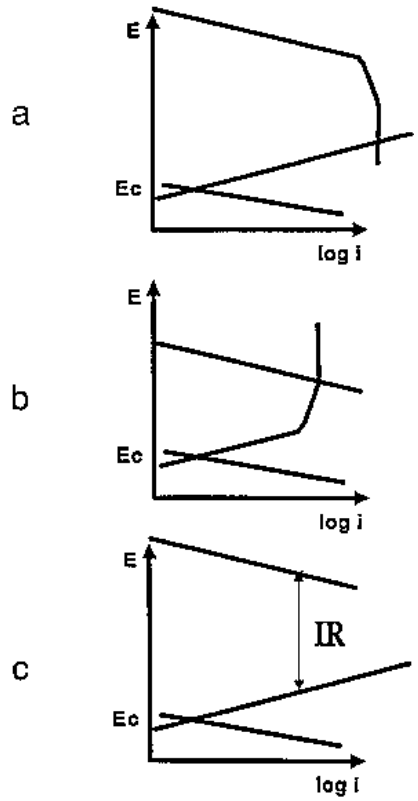

Figure 2.10: The limitation to pit growth shows in each Evan diagrams: (a) diffusion limitation at cathode, (b) salt film formation at anode, and (c) IR limitation between anode and cathode.

Source: Fontana (1967)

Pits always grow with a porous cover which can make visual detection extremely difficult, so that the awareness of the severity of attack is overlooked and the likelihood of catastrophic failure is enhanced. The pit cover might be a thick, precipitated product layer that forms as the concentrated and acidic pit solution meets the bulk environment, which might be neutral or limited in water, as in the case of atmospheric corrosion. Small pits in stainless steels often have apit cover that is a remnant of the undermined passive film (Frankel et.al., 1987).

The autocatalytic nature of pitting can be considered to be stable pitting which can stop growing or die. The pit will continue repassivate if the environment and potential at the dissolving wall of a pit are not sufficiently aggressive enough. The potential at the pit bottom is lower than that at the outer surface as a result of the ohmic potential drop associated with current flow out of the pit. There have increasing on the ohmic path length and ohmic resistance as the pit deepens. This tends cause an increase in the ohmic potential drop, a decrease in the pit current density. Since the hydrolysis of the dissolved metal cations and electrolytic migration of chloride into the pit, therefore the environment tends to be acidic and rich in chloride. The high concentration in the pit is depleted by transport out of the pit. The pit current density tends to decrease with time, owing to an increase in the pit depth and ohmic potential drop. Repassivation might occur if a sudden event, such as loss of a pit cover, caused a sudden enhancement of transport and dilution of the pit environment to the extent that the rate of dissolution at the pit bottom would be insufficient to replenish the lost aggressive environment (Frankel, 2006).

2.2.2 Pitting Potential

Stable pits form at potentials noble to the pitting potential, E_p and grow at potentials noble to the repassivation potential, E_R which is lower than $E_{p.}$ the effect of the potential on pitting corrosion and the meaning of these characteristic potentials show in the schematic polarization curve (Figure 2.11). This figure is a plot of the potential versus the logarithm of the current density. Potential is measured versus a reference electrode, commonly a saturated calomel electrode (SCE), and a potentiostat is used, along with an auxiliary or counter electrode, to make such measurements. As mentioned previously, current density is a measure of the rate of reaction.

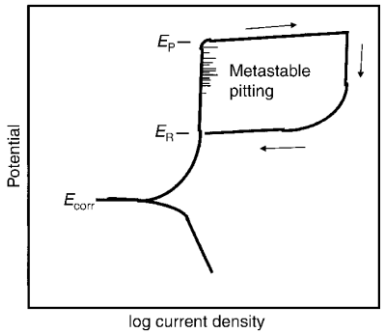

Figure 2.11: Schematic of polarization curve showing critical potentials and metastable pitting region. E_p, pitting potential; E_R, repassive potential; E_{corr}, corrosion potential

Source: Leckie and Uhlig (1996)

There are pitting corrosion forms when the potential exceeds acritical value E_p in the passive range of a polarization curve. E_p decreases with the concentration of the aggressive anions (Strehblow and Marcus). E_p (sometimes called critical potential or breakdown potential, E_B) above which stable pit initiate and grow up rapidly. For E_R, sometimes called protection potential, below growing pits repassivate and stop growing. Values of these two characteristic potentials can be measured by potential scan rate. Pitting corrosion can be influenced the evaluation of the both E_p and E_R. where the higher E_p and E_R are more resistant to pitting corrosion (Frankel, 1998).

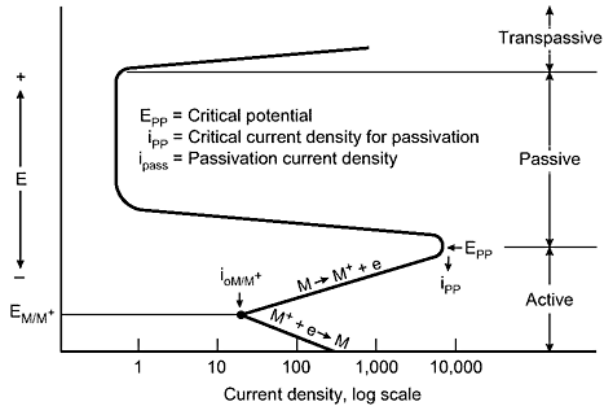

Figure 2.12: Typical anodic dissolution behaviour of an active – passive metal.

Source: Avallone et.al. (2007)

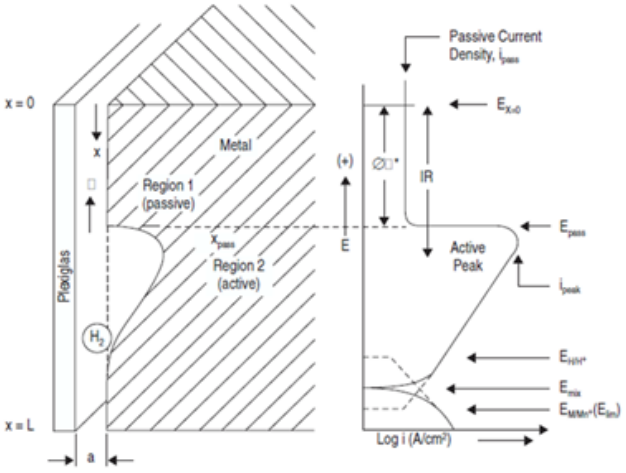

Figure 2.13: Schematic illustrations of the crevice corrosion attack on the crevice wall (left), and the IR-produced E(x) distribution and resulting i(x) current densities (skewed polarization curve) on the crevice wall (right).

Source: Shaw et.al. (2001)

Figure 2.12 and Figure 2.13 schematically show the variation of the anodic partial current density of a passivating metal as a function of the potential. The critical potential, E_{pp} or passivation potential, E_p separates the active from the passive potential region where the passivation current density, i_{pp} is the corresponding current density at the maximum. The i_{pp} characterizes the dissolution behaviour of the metal alloy in the passive potential region. The transpassivation potential E_b marks the end of the passive potential region and the transition from passive to transpassive behaviour. Beyond this point the anodic partial current density increases markedly with increasing potential due one of the following processes: uniform transpassive dissolution resulting from oxidation of the passive film, dissolution by pitting resulting from local breakdown, oxygen evaluation due to the water oxidation. When dissolution by pitting is the dominating reaction, the potential E_b is called critical pitting potential. It acts as film breakdown potential, which indicated that pitting is initiated by passive film breakdown. Depending on conditions, the value of E_b can be either above or below the reversible potential of the oxygen electrode, E_{rev,O_2}. For sufficiently stable passive films with good electronic conductivity, oxygen evolution rather than transpassive dissolution therefore account for the observed current at high anodic potentials (Avallone et.al., 2007).

As conclusion, a low value of E_b and a high value of E_p will get a good corrosion resistance of an alloy.

2.3 FACTORS INFLUENCING PITTING CORROSION

There are two factors influence pitting corrosion on aluminium alloys discussed in this part: effect of temperature and concentration of chloride solution.

2.3.1 Effect of Temperature on Pitting

Temperature is a critical factor in pitting corrosion. This is because many materials will not pit at a temperature below a certain value. The temperature dependence of an electrochemical reaction rate for pitting corrosion occurring on the surfaces of aluminium alloy is determined conventionally in two ways, which is recording controlled varying potentials (voltammetry) over a number of different temperatures and measuring current densities under constant temperature conditions (thermostatic). The CPT measured in concentrated chloride solutions, but they were independent of chloride concentration in the range 0.01 M–5 M and of pH in the range 1–7 (Shaw et.al., 2001).

Stable pitting obtains at temperatures above critical pitting temperature (CPT). Below this temperature, stable pitting does not take place at any potential which means by high breakdown potentials are observed, the corresponding to transpassive dissolution at low temperatures. Pitting corrosion only occurs at a potential that is below the transpassive breakdown potential when it is above this critical pitting corrosion (CPT). The pitting potential decreases with increasing temperature and chloride concentration at higher temperatures. CPT is associated with the dual role of a salt film in either stabilizing pit growth by providing a buffer of solute (at high temperatures) or facilitating repassivation (at low temperatures). There are a range of critical pitting temperatures for many stainless steels, which is around 10-100 ℃. CPT can be used for ranking susceptibility to pitting corrosion; the higher the CPT, the more resistant the alloy to pitting. On the other hand, aluminium alloys do not exhibit a CPT in aqueous chloride solutions at temperatures down to 0 ℃ (Zhang et.al., 2009).

2.3.2 Effect of Chloride Ions Concentration

Corrosion of aluminium occurs when the metal protective oxide layer is damaged and the repair mechanism is prevented by chemical dissolution. In the presence of chloride ions, the passive film breaks down at a specific potential identified as $E_{b,pit}$ at which there is rapid increase in current density. The polarization curve become the large-dashed curve when the chloride concentration is sufficiently high to complete prevent passivation. Increase in pH changed the slope of the cathodic polarization curve by changing the cathodic reaction. Increasing the chloride ion concentration decreased the cathodic reaction rate. The anodic reaction rate increased with increase in chloride ion concentration. The open circuit corrosion potential and the pitting potential shifted in the active (negative) direction with increasing pH and chloride ion concentration (Ambat and Dwarakadasa, 1993). The curves show in Figure 2.14.

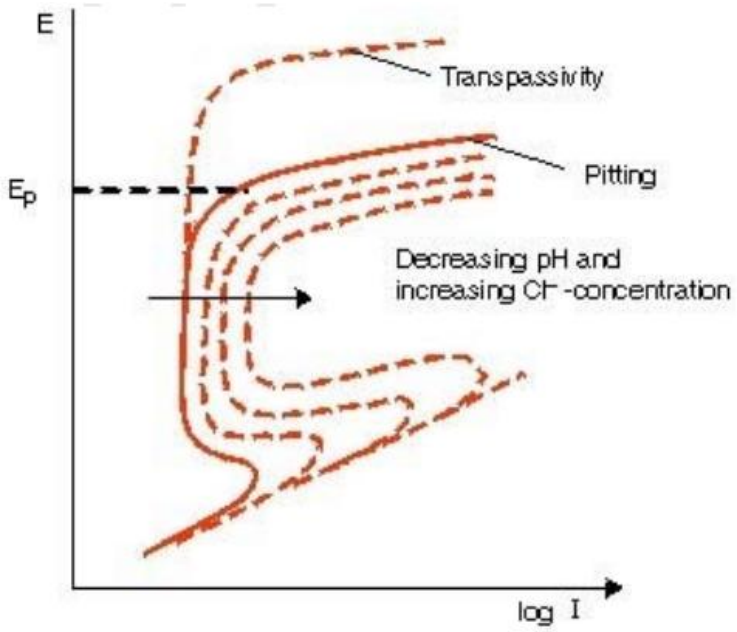

Figure 2.14: Schematic anodic overvoltage curves for an active-passive metal or alloy.

Source: Corrosion in Seawater - Biological Effects. E. Bardal *Norwegian University of Science and Technology, Norway*

Potentiodynamic polarization curves for both the alloys are shown in Figure 2.15 for pH values of 6.0. Except for AA2014 at pH6.0, all the curves exhibited an apparent active region, with passivity at intermediate values of potential and pitting at and beyond the pitting potential. Increase in chloride ion concentration shifted the intersecting point of the cathodic and anodic curve (E_{corr}) in the active (negative) direction. Increase in chloride ion concentration shifted the passive region of the anodic curve to higher current density values. Increase in chloride ion concentration decreased the cathodic reaction rate, but the slope of the curve remained almost the same.

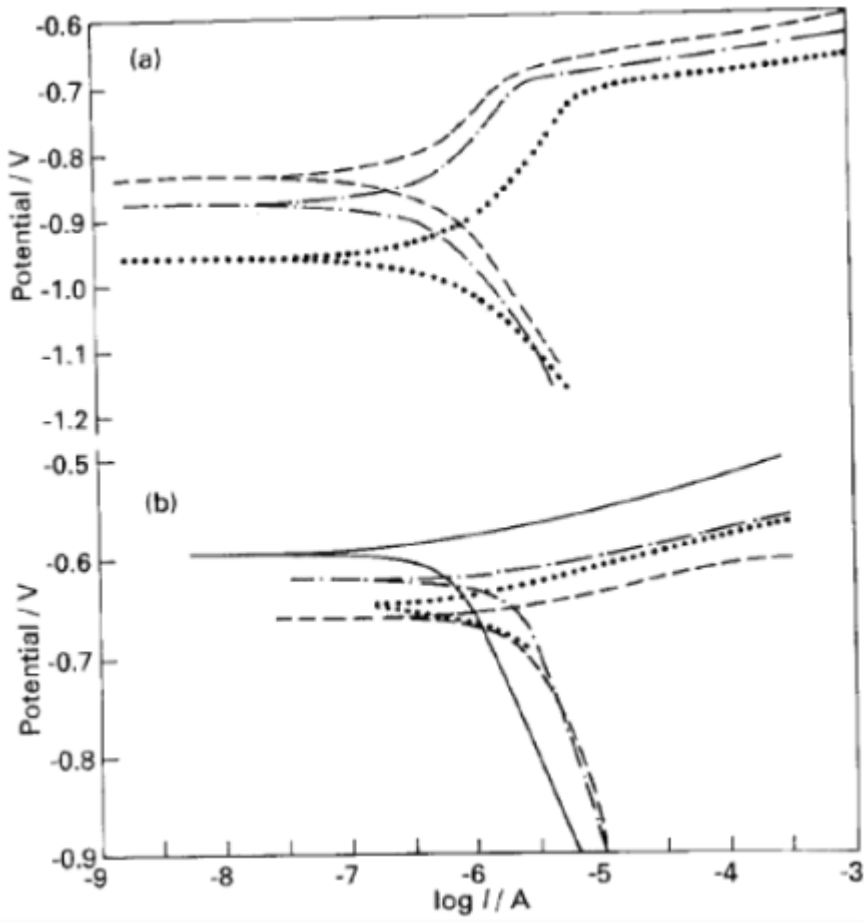

Figure 2.15: Potentiodynamic polarization curves for various alloys at pH 6.0 in NaC1 solution of different concentrations. (a) 8090-T851 and (b) 2014-T6: (−) 1.0, (-- -) 3.5, (- . -) 5.0 and (. . .) 10 wt %.

Source: Ambat and Dwarakadasa (1993)

2.4 ELECTROCHEMICAL CORROSION MEASUREMENT

Polarization Resistance and Tafel Plots are experiments designed to measure the rate of uniform corrosion in units of penetration (mmpy or mpy). Designed to measure the corrosion current, I_{corr} is used to calculate the corrosion rate.

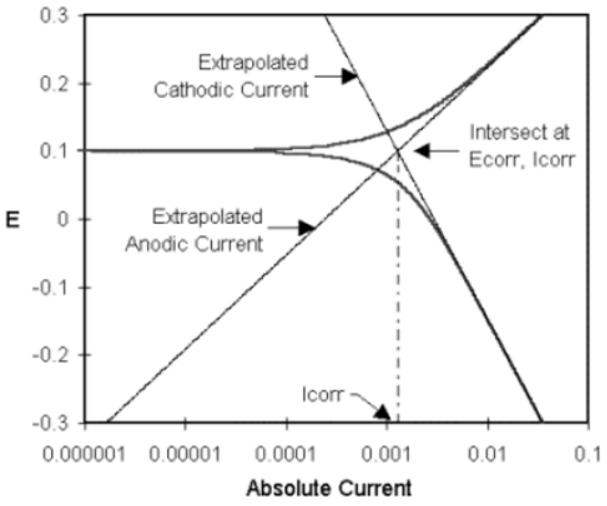

Figure 2.16: Classic Tafel Analysis

Source: Application Note - Camry Instrument

Polarization method is commonly used for detecting the corrosion rate and the deterioration of coatings. The corrosion current density (I_{corr}) can be calculated through equation 2.4:

$$\boldsymbol{R_{corr}} = \frac{\boldsymbol{\beta_a \beta_c}}{\boldsymbol{2.303\, I_{corr}(\beta_a + \beta_c)}} \qquad \text{Equation 2.4}$$

β_a and β_c are Tafel constants which can be obtained from a well-known Tafel plots for the system under consideration. The corrosion rate of the structure can be calculated through I_{corr} showed as equation 2.5

$$\boldsymbol{CR} = \frac{\boldsymbol{(I_{corr}\, KEW)}}{\boldsymbol{dA}} \qquad \text{Equation 2.5}$$

where,

CR = Corrosion rate, units are given by the choice of K

I_{corr} = Corrosion current in amps

K = 3.45 x 10^6 (for CR in Mpy)

=8.75 x 10^4 (for CR in mmpy)

EW = Equivalent weight in grams/equivalent

d = Density in grams/cm^3

A = Sample area in cm^2

For the weight loss corrosion rate, it shows in equation 2.6 below:

$$\boldsymbol{CR} = \frac{\boldsymbol{W\ x\ K}}{\boldsymbol{D\ x\ A\ x\ T}} \qquad \text{Equation 2.6}$$

CR = Corrosion rate, units are given by the choice of K

K = 3.45 x 10^6 (for CR in Mpy)

= 8.75 x 10^4 (for CR in mmpy)

W = Weight loss in grams

D = Density in gram/cm^3

A = Sample area in cm^2

T = Exposed time in hours

2.5 MATERIAL

There are many series of aluminium alloys. Each series will discuss in the chapter for further works.

2.5.1 Types of Aluminium Alloys

There are many types of aluminim alloys to presnet. For Table 2.1 shows that the main alloying elementsin wrought alloy designation system and Table 2.2 is explanation for main features of some marine grade aluminium alloys (series 5000 and 6000) and a few others for reference.

Table 2.1: Main Alloying Elements in Wrought Alloy Designation System

Alloy	Main Alloying Element
1000	Mostly pure aluminium; no major alloying additions
2000	Copper
3000	Manganese
4000	Silicon
5000	Magnesium
6000	Magnesium and silicon
7000	Zinc
8000	Other elements (e.g., iron or tin)
9000	Unassigned

Source: Kaufman (2007)

2.5.1.1 Effect of Alloying Elements

i. **1000 Series:** Aluminium of 99% or higher purity has many applications in the electrical and chemical fields. These alloys are characterized by excellent corrosion resistance, high thermal and electrical conductivity, low mechanical properties, and excellent workability. Moderate increases in strength may be obtained by strain hardening. Iron and silicon are the major impurities.

ii. **2000 Series:** Copper is the principal alloying element in this group. These alloys require solution heat-treatment to obtain optimum properties: in the heat-treated condition mechanical properties are similar to and sometimes exceed those of mild steel. In some instances artificial ageing is employed to further increase the mechanical properties. This treatment materially increases yield strength, with attendant loss in elongation; its effect on ultimate tensile strength is not as great. It does not have as good corrosion resistance and under certain conditions they may be subject to inter-granular corrosion.

iii. **3000 Series:** Manganese is the major alloying element of alloys in this group, which are non- heat treatable. Because only a limited percentage of manganese,

up to about 1.5%, can be effectively added to aluminium. These are popular and are widely used as general-purpose alloys for moderate-strength applications requiring good workability.

iv. **4000 Series:** The major alloying element of this group is Silicon, which can be added in sufficient quantities to cause substantial lowering of the melting point without producing brittleness in the resulting alloys. For these reasons aluminium-silicon alloys are used in welding wire and as brazing alloys where a lower melting point than that of the parent metal is required. Most alloys in this series are non-heat treatable, but when used in welding heat-treatable alloys they will pick up some of the alloying constituents of the latter and so respond to heat treatment to a limited extent. The alloys containing appreciable amount of silicon become dark grey when anodic oxide finishes are applied.

v. **5000 Series:** Magnesium is one of the most effective and widely used alloying elements for aluminium. It is a moderate to high- strength non-heat treatable alloy. Magnesium is considerably more effective than manganese as a hardener, about 0.8% magnesium being equal to 1.25% manganese, and it can be added in considerably higher quantities. Alloys in this series possess good welding characteristics and good resistance to corrosion in marine atmospheres. However, certain limitation should be placed on the amount of cold work and the safe operating temperatures permissible for the higher magnesium content alloys to avoid susceptibility to stress corrosion and exfoliation attack.

vi. **6000 Series:** Alloys in this group contain silicon and magnesium in approximate proportions to form magnesium silicide, thus making them capable of being heat-treated. Though less strong than most of the 2000 or 7000 alloys, the magnesium-silicon (or magnesium-silicide) alloys possess good formability and corrosion resistance, with medium strength. Alloys in the heat-treatable group may be formed in the T4 temper (solution heat-treated but not artificially aged) and then reach full T6 properties by artificial ageing.

vii. **7000 Series:** Zinc is the major alloying element in this group, and when coupled with a smaller percentage of the magnesium results in heat-treatable alloys of very high strength. Usually other elements such as coppers and chromium are also added in small quantities.

2.5.2 AA6061-T6 Aluminium Alloy

Aluminium, copper and titanium alloys are the most important of the alloys belonging to the group of non-ferrous metals which used in marine engineering (Jerzy and Igor, 2007). Pure aluminium is soft and weak, but it can be alloyed and heat-treated to a board range of mechanical properties. Table 2.3 shows some properties of selected aluminium alloy. Aluminium alloys are alloys in which aluminium (Al) is the predominant metal. The typical alloying elements are copper, magnesium, manganese, silicon and zinc. There are two principal classifications, namely casting alloys and wrought alloys, both of which are further subdivided into the categories heat-treatable and non-heat-treatable.

AA6061-T6 has moderate strength but excellent weldability compared to other heat treatable alloys, excellent corrosion resistance and a high plane strain fracture toughness. AA6061 will age naturally to an essentially stable T4 condition. The softer conditions can be preserved by refrigeration. The formability of the "O" condition can be preserved for 2 hours at room temperature, 2 days at 0 ℃, and 7+ days or more at -7 ℃. Figure 3.2 shows the composition limit for this material. AA6061 is an versatile heat treatable aluminum alloy. AA6061 has a wide range of mechanical and corrosion resistance properties as well as having most of the good qualities of aluminium. AA6061 is used in a many applications from aircraft structures, yacht construction, truck bodies, bicycle frames to screw machine parts.

Table 2.2: Properties of selected Aluminium Alloys

Alloy	Temper	Wrought /Cast	Density	Electrical Conductivity (% IACS)	Yeild Strenth (Mpa)	Tensile Strength (MPa)	Elongation (%)
1199	O	W	2.71	60	10	45	50
3003	H14	W	2.73	50	145	152	8
5005	H38	W	2.7	52	200	186	5
5052	H38	W	2.68	35	290	255	7
2024	T861	W	2.77	30	490	517	6
6061	T6	W	2.71	43	276	310	12
7075	T6	W	2.8	22	503	572	11
	T73	W			434	503	13
201	T4	C(sand cast)	2.8	30	215	365	20
356	T51	C(sand cast)	2.69	41	140	175	2
413	F	C(die cast)	2.66	39	140	300	2.5

Sources: (Jerzy and Igor, 2007)

Table 2.3: The following table gives main features of aluminium and AA 6061-T6

Aluminum Grade-Temper	General	Yield strength (psi)	Ultimate Tensile Strength (psi)	Work ability	Weld ability	Hardness (Brinell)	Chemistry
Pure Al 1xxx Series	Low strength (soft), non-magnetic, highly electrically and thermally conductive, high corrosion resistance. Used for wrought aluminum elements.	24,000	29,700			12-55	Al 99.0% min
6061-T651	Marine grade, often used to build boat hulls and other components. The most often used aluminum alloy for its strength, heath treatability, workability and weldability.	40,000	45,000 17%	Good	Good	95	Al 95.8-98.6% Cr 0.04-0.35% Cu 0.15-0.40% Fe 0.70% Mg 0.8-1.2% Mn 0.15% max Si 0.4-0.8% Zn 0.25%

Source: You Boat.net

CHAPTER 3

METHODOLOGY

3.1 INTRODUCTION

In this study, the present work is aimed to investigate the effect of some variable on the pitting corrosion behaviour on AA6061-T6 aluminium alloy and study their electrochemical behaviour in NaCl solution using polarization technique. In order to study the electrochemical behaviour of pitting behaviour of the as-received material, different concentration (3.5 wt%, 4.5 wt%, 5.5 wt%) and temperatures (25℃, 35℃, 45℃, 55℃, 65℃) NaCl concentration solutions test in this study. A flow chart will be used to indicate the flow of the whole study was shown in Figure 3.1. The result of the compositional analysis of the as-received sample (AA 6061-T6) is showed in this chapter which will determine the amount of content of elements in the material.

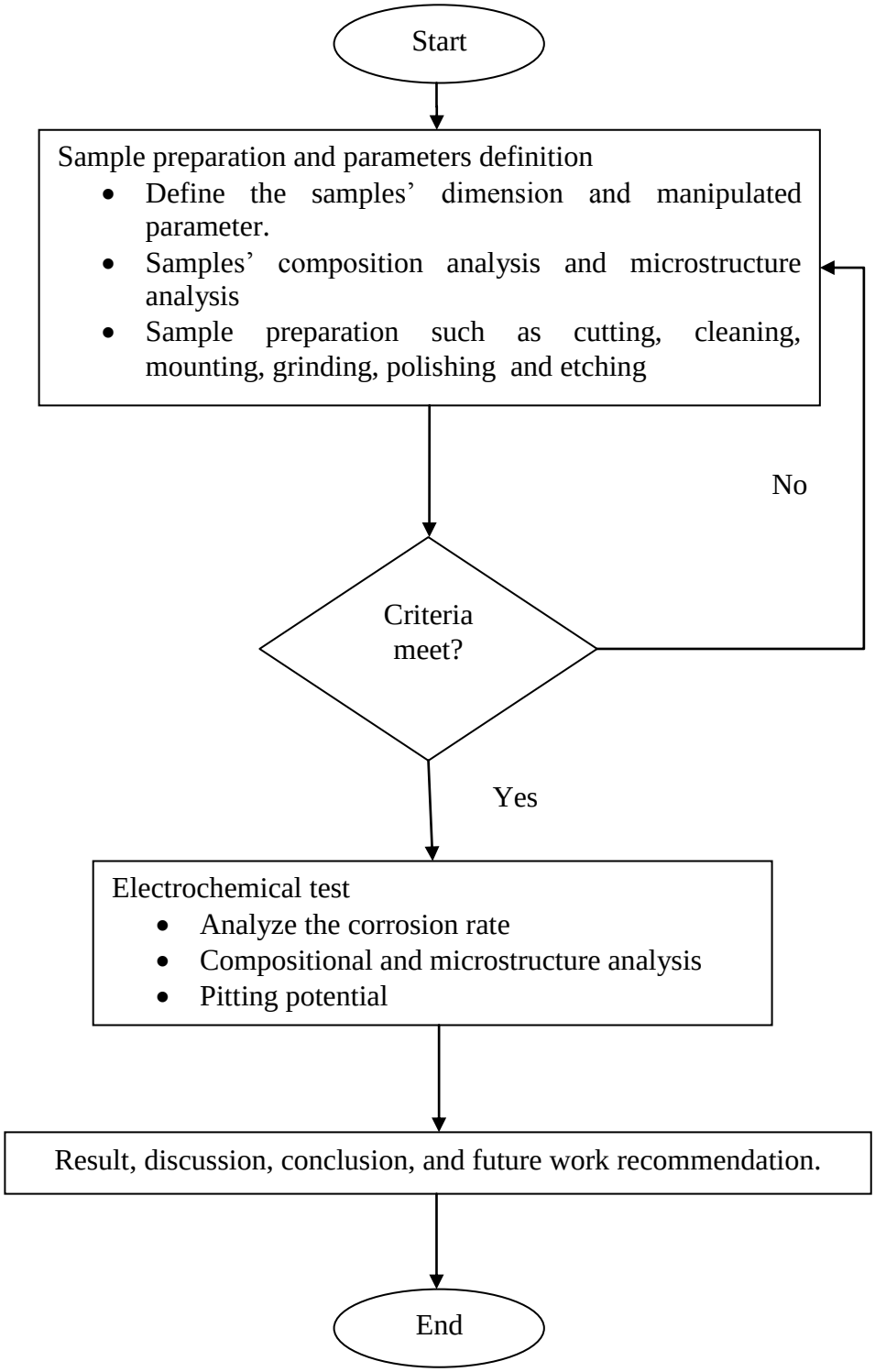

Figure 3.1: A flow chart showing a summary of the research methodology

3.2 SAMPLE PREPARATION

This experiment ran on material of AA6061-T6 by using electrochemical test. The sample material was cut into the desired size using the shearing machine (MSV–C 31/6) as shown in the Figure 3.2. From the workpieces of AA6061-T6, the composition was analyzed at the foundry lab of FKM in UMP Pekan. Figure 3.3 shows the sample with thickness of 3 mm which is cut in 3 cm x 6 cm by using the shearing machine.

Figure 3.2: Shearing machine (MSV-C 31/6)

The samples after that were cut into small pieces with dimension of 2 cm x 1 cm as shown in Figure 3.3. Therefore, the sectional cut off machine as shown in Figure 3.4 was used in cutting process. During this cutting process, coolant must be applied along the cutting process to produce a good surface finish. The cutting speed of the cutter was low in order not to alter or affect the surface of the sample and minimized the effect of the heat due to the cutting process.

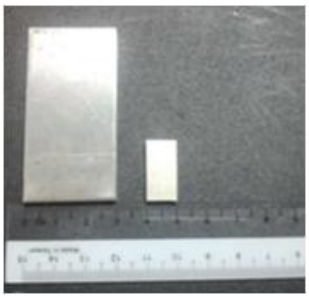

Figure 3.3: Sample after shearing process and cutting process

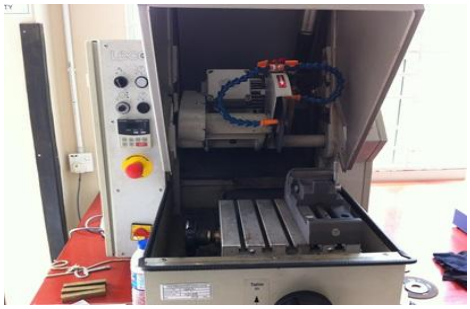

Figure 3.4: Sectional cut-off machine

3.3 METALLOGRAPHIC ANALYSIS

Microstructure analysis discussed on the topics of the sample before and after they corrode. Process of cutting, shearing, grinding, polishing, and etching were carried out before the microstructure analysis was performed in order to produce high surface finish and clear microstructure. The specimens were ground to produce a plane surface with minimal scratches and polishing to obtain a mirror-like surface which will produce clear and minimal scratch microstructure.

First, the sample was connected with a copper wire by using the insulation tape as shown in Figure 3.5. This connection was important in the electrochemical test in order to analyse the corrosion rate that occurred on the surface of the specimen. A voltmeter (Figure 3.6) used to check the current after the sample was connected with copper wire.

Figure 3.5: Sample connected with copper wire by using insulation tape

Figure 3.6: Voltmeter

Next, the sample proceeded with cold mounting process. Cold mounting process was done in order to support and hold the sample during microstructure analysis. Cold mounting process can be done using LECOSET 7007 as shown in Figure 3.7 and fill the mould in the LECOMAT pressure vessel at approximately 2 bars pressure (Figure 3.8). LECOSET 7007 is a rapid cold curing acrylic designed for any lab needing fast, dependable and reproducible results which is a two- part cold polymerization which required a combination of resin and liquids. Ratio of 2 : 1 for the resin and liquid was measured by using the moulding cup (Figure 3.9) when high abrasion resistance and superior edge retention is required. The cure time for this process was 10 to 15 minutes and forms an opaque white mount as shown in Figure 3.10 that resists most cleaning fluids and etching reagents (clear if under pressure).

Figure 3.7: LECOSET 7007 (resin and liquid)

Figure 3.8: Cold Mounting Machine

Figure 3.9: Mounting cup

(a) **(b)**

Figure 3.10: Finishing sample (a) bottom view (b) top view

Table 3.1: A typical ceramographic grinding and polishing procedure for the grinding and polishing machine

Step	Abrasive and lubricant	Time/sec	Wheel speed/rpm	Pressure /psi
Grinding	SIC 320 grit	60	300	40
	SIC 400 grit	60	300	40
	SIC 600 grit	60	300	40
Polishing	Red felt cloth with 6 micron diamond suspension and microid extender	300	250	30
	Imperial cloth (watted) with 0.05 micron colloidal silica	60	150	15

Continue by the grinding and polishing processes to which can produce a minimal scratches plane surface and mirror like surfaces. Grinding is a process carried out with a grinding wheel made up of abrasive grains for removing very fine quantities of material from the workpieces surface. The purpose of grinding is to lessen the depth of deformed metal to the point where the last leftovers of damage can be removed by sequence of polishing steps. The sample was ground in three level of silicon carbide waterproof abrasive paper which located on the four tracks of grinding machine as shown in Figure 3.18. The sample must be only ground in one direction either upward or downward to have a flat plane.

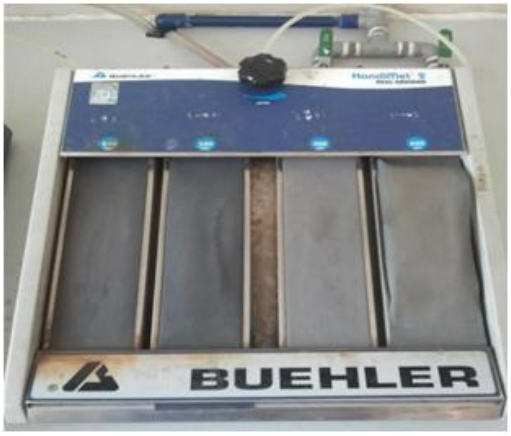

Figure 3.11: Manual grinding machine

After grinding process, polish the samples on polishing cloths loaded with lubricant and progressively smaller diamond abrasives. In the Table 3.1 showed that the different type of diamond suspension, colloidal silica and microid extender used in the polishing machine (Figure 3.13). The polishing lubricant adhered the abrasive and swarf to the paper to prevent dust, enables the abrasive particles to roll and slide easily between the paper and the specimen, and uniformly distributes the contact stresses between the paper and the sample during polishing.

Figure 3.12: Polishing machine

(a) (b)

Figure 3.13: (a) Microid extender and (b) 6 micron diamond suspension for red felt cloth

Figure 3.14: 0.05 micron colloidal silica for imperial cloth (watted)

Before the sample observing by microscope, there was an etching process in order to reveal the grain boundaries of the microstructure by using the etchant liquid for aluminium alloy (Figure 3.15). The sample must be clean with the distilled water in order to prevent corrosion process happened.

Figure 3.15: Etching solution

Finally, the samples were observed under an optical microscope as shown in Figure 3.16 with magnification of x50 in order to get a clear vision microstructure.

Figure 3.16: Optical microscope

3.4 COMPOSITIONAL ANALYSIS

In this part, the spectrometer Foundry-Master UV in the foundry lab was used to analyze the compositional analysis of the as-received sample. Figure 3.17 showed the spectrometer machine. The sample was analyzed in order to get its average compositional analysis values. The type and grade of the material can be identified by comparing to the standard value of the elements of the material based on the amount of content of elements in the material. The sample must undergo the grinding process before the compositional analysis, in order to remove the coating layer.

Figure 3.17: Spectrometer Foundry-Master UV machine

Figure 3.18: Sample as-received material

The spectrometer Foundry-Master UV was used to analyze the compositional analysis of the as-received sample determined the amount of content of elements in the sample. The compositional analysis of the as-received sample and the standard compositional analysis of AA6061-T6 based on Appendix A2 are shown in Table 3.2. Type and grade of material AA 6061-T6 can be identified based on the amount of content elements in the as-received material.

Table 3.2: Composition analysis of as-received material

Material	**Element, Alloy weight (%)**									
	Al	**Si**	**Fe**	**Cu**	**Mn**	**Mg**	**Cr**	**Zn**	**Ti**	**Others**
As-received sample	97.2	0.8	0.4	0.2	0.1	0.8	0.2	0.05	0.05	0.20
Standard AA6061-T6	Bal	0.4-0.8	0.7	0.15-0.40	0.15	0.8-1.2	0.04-0.35	0.25	0.15	0.20

From the data of Appendix A2 which showed in Table 3.1, there are only four type aluminium alloys consist Cr and Ti. Table 3.2 showed the alloy weight of silicon in the composition analysis of as-received material has 0.8 % alloy weight. This value only matchs with AA6061-T6 aluminium alloy. Although the percentage of iron content of the as-received material is less than 0.3 % of the standard AA 6061 –T6, but the percentage of copper, magnesium and chromium contents are in the range.

Alloy weights of manganese is the sample only has 0.1 % which is less than 0.05 % than the standard values. Same cases are happen on the alloy weight of zinc and

titanium, they only have 0.05 % in each group. But, content of zinc is 0.25 % in alloy weight where the titanium has 0.15%.

Standard AA 6061 – T6 is the only one material that consist Cr and Ti with element Si as high as 0.8 % alloy weight, but based on the amount of contents of silicon, copper, magnesium and chromium in the sample as shown in Table 4.1, the type and grade of this sample can be identified as aluminium alloy 6061 – T6.

3.5 ELECTROCHEMICAL TEST

By the potentiodynamic anodic polarization using Potentiostat Galvanostat instrument (Figure 3.19), an electrochemical corrosion test is carried out. From Figure 3.20 showed the setup of this experiment where the Table 3.3 has been mentioned all the parameter in the electrochemical test. Figure 3.19 showed an equipment which named as WPG – 100 potentiostat was used in this experiment. The corrosion potential (E_{corr}) and corrosion current density (I_{corr}) can be estimated from the curve data fitting of the standard model given.

Table 3.3: Parameter setup in electrochemical test

Parameter	Unit
Initial voltage, E	-1.5 V
Final voltage, E	1.5 V
Scan rate	8 mV/s
Sampling time	375 s
Sample area	2 cm^2
Density	2.7 gm/cm^3
Equivalent weight	9.01
Condition time	0 s
Condition E	0 V
Condition I	0 A
Initial delay	10 S
Delay limit	0.1 mV/S
Working electrode	AA6061-T6
Counter electrode	Graphite
Reference electrode	Saturated colomel electrode (SCE)

The experiment carry out under static condition at different concentration of solutions which is (3.5, 4.5 and 5.5 wt%) of NaCl at room temperature. The synthetic seawater has a salinity of about 3.5 wt% which means 35 g of sodium chloride solutes in 1 L of distilled water. For the 4.5 wt% and 5.5 wt% of solution, there are 45 and 55 gram of sodium chloride mix with 1 litre of distilled water to produce 1 litre of solution NaCl with concentration of 4.5 wt% and 5.5 wt%.

The procedures above are repeated with different temperature which have 25 ℃, 35 ℃, 45 ℃, 55 ℃, 65 ℃ and 75 ℃ in synthetic seawater (3.5 wt % NaCl) by using the Memmert water bath showed in Figure 3.21. The Memmert water bath is used to control the temperature of test solution when undergoes pitting corrosion experiment. This equipment first is filled in the distill water into the bath. The setup of electrochemical put into the bath and temperature of solution controlled by water bath machine. A thermometer is used to measure temperature of the solution's temperature. Table 3.4 shows the condition of each experiment.

Table 3.4: Manipulated Parameter

Sample	Temperature, ^{o}C	Concentration of NaCl, wt%
1	Room temperature	3.5
2	Room temperature	4.5
3	Room temperature	5.5
4	25	Synthetic seawater
5	35	Synthetic seawater
6	45	Synthetic seawater
7	55	Synthetic seawater
8	65	Synthetic seawater

Figure 3.19: WPG-100 Potentiostat equipment

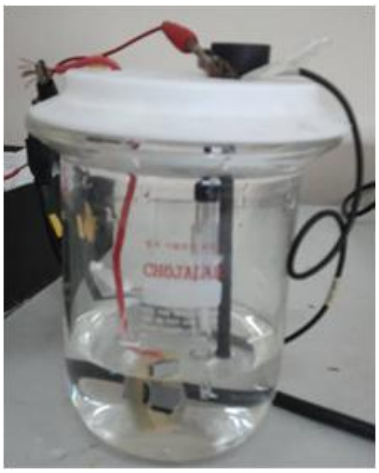

Figure 3.20: Electrochemical measurement setup

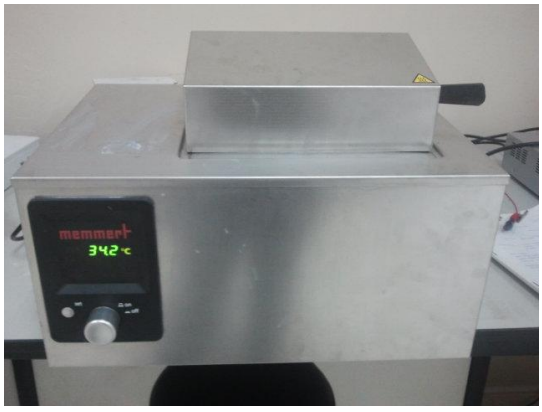

Figure 3.21: Water Bath

3.6 WEIGHT LOSS METHOD

One immersion test method for pitting corrosion has run, where the samples are immersed in different concentration (3.5, 4.5 and 5.5) %wt solution NaCl. This solution is corrosive due to the simultaneous presence of chloride ions and oxidising sodium ions. The temperature is held in room temperature and the recommended time for exposure is two months. After cleaning, the samples are weighed and the surfaces are examined for pits. By using weight loss corrosion rate formula (equation 2.6), the corrosion rate of this experiment can be calculated. The data of three samples has been collected on table 3.5. This data can use to compare with the potentiodynamic experiment.

Figure 3.22: Natural pitting experiment

Table 3.5: Manipulated Parameter

Sample	Temperature, ^{o}C	Concentration of NaCl, wt%
9	Room temperature	3.5
10	Room temperature	4.5
11	Room temperature	5.5

The experimental flow chart in Figure 3.23 is a visual representation of the sequence of the weight loss method. A completed flow chart organizes the topic to ensure that the smoothing flow of this experiment.

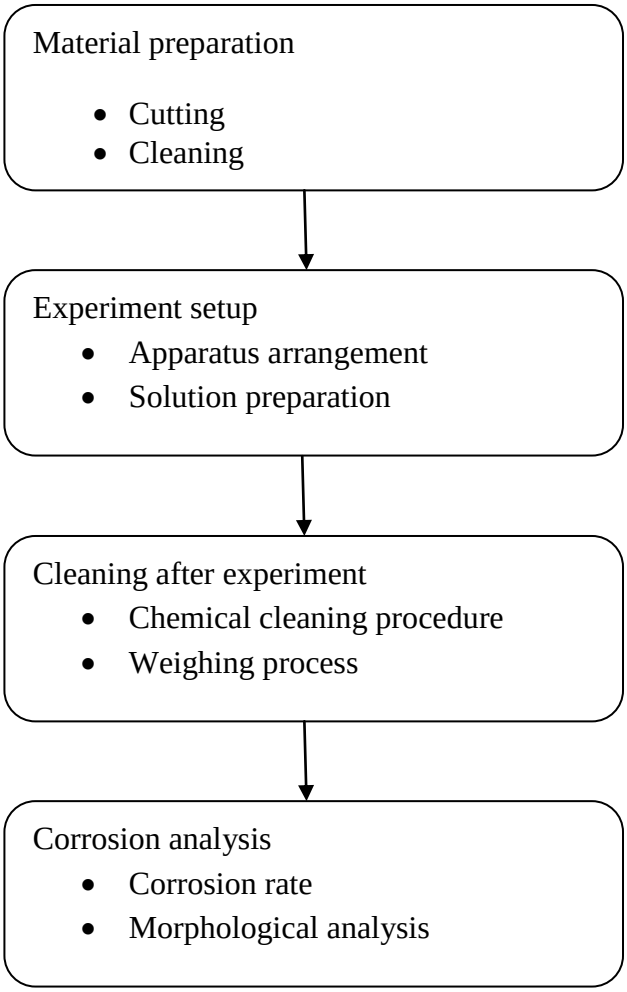

Figure 3.23: Experimental flow chart for weight loss method

3.7 SCANNING ELECTRON MICROSCOPE

Scanning electron microscope (SEM) uses a focused electron probe to extract structural and chemical information point-by-point from a region of interest in the sample. The high spatial resolution of an SEM makes it a powerful tool to characterise a wide range of specimens at the nanometre to micrometre length scales.

The SEM in material lab of Faculty of Manufacturing Engineering UMP used to analyze the microstructure of each sample. Figure 3.24 showed the PHENOMWORLD SEM and figure 3.25 showed the preparing setup before analyzed by using SEM.

.

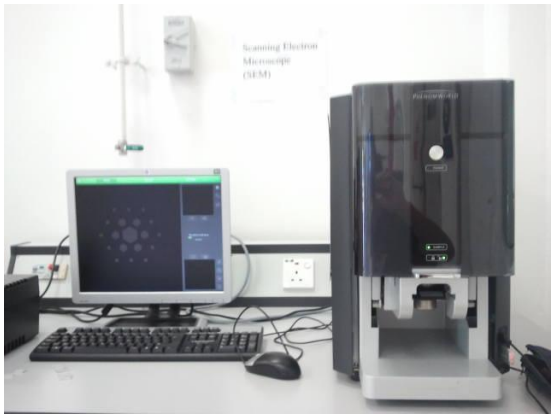

Figure 3.24: PHENOMWORLD Scanning electron microscope

Figure 3.25: Preparation before analyzed by using SEM

CHAPTER 4

RESULT AND DISCUSSION

4.1 INTRODUCTION

The present work aims to study the results of the influence of temperature (25 ℃, 35 ℃, 45 ℃, 55 ℃, 65 ℃ and 75 ℃) and concentration of NaCl solution (3.5, 4.5 and 5.5 wt%) on the pitting corrosion of AA6061-T6 aluminium alloy by using polarization method. The results of polarization diagrams of the eleven samples during the test carried out in different temperature and concentration are discussed. All the data which get from the test will type in tables. Electrochemical measurement is used to analyze the corrosion of AA6061-T6. The corrosion rate will be calculated automatically by using IV Man software.

Weight loss experiment for the different concentration experiment has been run in the same time to compare the results with electrochemical tests. The results of this experiment will be compared with the electrochemical experiment in this chapter.

On the other hand, the effects of each parameter on the corrosion behaviour of aluminium alloy 6061-T6 are discussed in this part. The microstructure of samples checked by using optical microscope in order to detect the corrosion product and the types of the corrosion defect occurred after corrosion test has been run.

4.2 POLARIZATION RESULTS OF ELECTROCHEMICAL TEST

Potentiodynamic method which involves a continuous change of potential at a constant rate of 8mV/sec. It records the corresponding current density. Table 4.1 shows that the Tafel polarization data of sample 1, 2 and 3 for the different concentration of solution NaCl (3.5, 4.5, 5.5%wt) at room temperature under static condition. Parameter setup of the electrochemical test is shown in Table 3.3 (section 3.6). Different polarization diagrams are obtained by using Wontech WPG 100 potentiostat.

Tafel analysis is performed by extrapolating the linear portions of a logarithm of absolute current density versus corrosion potential plot back to their intersection. This diagram is performed by using the software which named as IV Man. Values of E_{corr} and i_{corr} can be determined by using extrapolated linear sections from the anodic and cathodic curves in Tafel analysis polarization diagram. E_{corr} and i_{corr} values can be directly determined from the cross-over point. The corrosion behaviour of the different concentration test samples were determined by Tafel analysis polarization diagram. At the corrosion potential, Ec_{orr}, rate of cathodic reduction is equal to rate of anodic reaction (metal corrosion). Tafel constants (β_a and β_c) are calculated from the anodic and cathodic slopes. Table 4.1 collected all the Tafel polarization data for the different concentration of solution NaCl.

Table 4.1: Tafel polarization data of different concentration of solution NaCl

Sample	E_{corr}, mV	I_{corr}, µA	i_{corr}, µA/cm ^{2}	β_A, V/dec	β_C, V/dec	CR, mpy	CR, mmpy
1	-1103	20.81	10.405	0.3180	0.1549	6.020	0.1529
2	-1148	44.78	22.39	0.7158	0.1598	9.264	0.2445
3	-1162	66.85	33.425	2.2920	0.1411	14.370	0.3650

Figure 4.1 shows that there slightly different for corrosion potential rate in each concentration. Based on Table 4.1, sample 3 showed the highest value of i_{corr} which is 33.425 µA/cm ^{2} while sample 1 had the lowest value of i_{corr} which is 10.405 µA/cm ^{2}. Sample 1 got the highest corrosion potential rate of -1103 mV where sample 3 had a result with the values of -1162 mV. Due to the relationship that i_{corr} is directly

proportional to the corrosion rate as shown in Equation 2.5 which discussed in section 2.4, the highest value of i_{corr} will lead to get the highest corrosion rate. Figure 4.4 shows that the graph of corrosion rate versus concentration solution of samples 1, 2 and 3. Based on Table 4.1, corrosion rate increases for 60% when the concentration of NaCl increases from 3.5 wt% to 4.5 wt%. For the sample 3, the corrosion rate increased for 0.1205 became 0.3650 mmpy compare with the corrosion rate for sample 1. Therefore, it can be concluded as the corrosion rate affected by the concentration of solution NaCl.

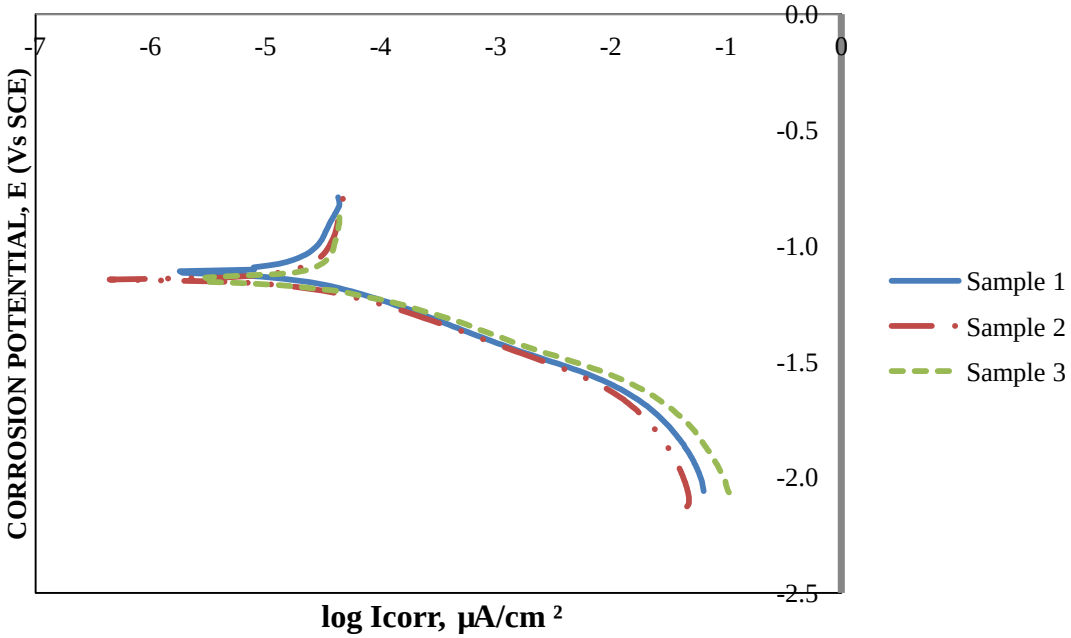

Figure 4.1: Polarization graph of different concentration solution

By referring to Table 4.2, sample with five different values of temperatures which test in 3.5%wt of NaCl are analyzed. From the Tafel polarization data of Table 4.3, sample 8 exhibits the highest value of i_{corr} and E_{corr} which have 110.3 µA/cm ²and -1189 mV. The sample 4 which test in 25 ^{o}C had -1103 mV for E_{corr} and 10.4053 µA/cm ² for i_{corr}. It is the lowest values obtained in this set experiment. Since that that i_{corr} is directly proportional to the corrosion rate as shown in Equation (2.5) which discussed in section 2.4, the highest corrosion rate will always occur at the highest value of i_{corr}.

When temperature of solution NaCl is 25^{o}C, the corrosion rate only had 0.1529 mmpy. This value had been increased for 0.1214 become 0.2743 mmpy when the temperature reached 35 ^{o}C. Corrosion rate of sample 6 when temperature continued heat until 45 ^{o}C increased 108.1 % compared with the previous sample. The corrosion rate keep increased until 0.724 mmpy at 55^{o}C. For the sample 8, its corrosion rate increased for 66.4% compare with the corrosion rate of sample 7. Thus, the corrosion rates of AA6061-T6 influenced by the increasing of temperature of electrolyte solution.

Table 4.2: Tafel polarization data of different temperature of solution NaCl

Sample	E_{corr}, **mV**	I_{corr}, **µA**	i_{corr}, **µA/cm ²**	β_A, **V/dec**	β_C, **V/dec**	**CR, Mpy**	**CR, mmpy**
4	-1103	20.81	10.405	0.3180	0.1549	6.020	0.1529
5	-1124	50.24	25.12	1.529	0.1541	10.08	0.2743
6	-1141	104.6	52.3	0.9114	0.1619	22.47	0.5708
7	-1160	132.6	66.3	0.7552	0.1587	28.5	0.724
8	-1189	220.6	110.3	1.117	0.1627	47.41	1.205

$$\boldsymbol{CR} = \frac{(\boldsymbol{Icorr\ KEW})}{\boldsymbol{dA}} \qquad \text{Equation 2.5}$$

CR – Corrosion rate, mm / year

I_{corr} – Corrosion current in amps

K – 3272, mm/amp*cm*year

EW – Equivalent weight in grams/equivalent

d – Density in gram/cm ³

A – Sample area in cm ²

ASTM Standard G 102, Standard Practice for calculation of corrosion rate

For example,

EW = 9.01

d = 2.7 g/cm ²

A = 2 cm ²

I_{corr} = 220.6 x 10^{-6} A (Sample 8)

$$CR = \frac{(Icorr\ KEW)}{dA}$$

$$= \frac{(220.6\ x\ 10^{-6}\ x3272x\ 9.01)}{(2.7\ x\ 2)}$$

$$= 1.205\ mmpy$$

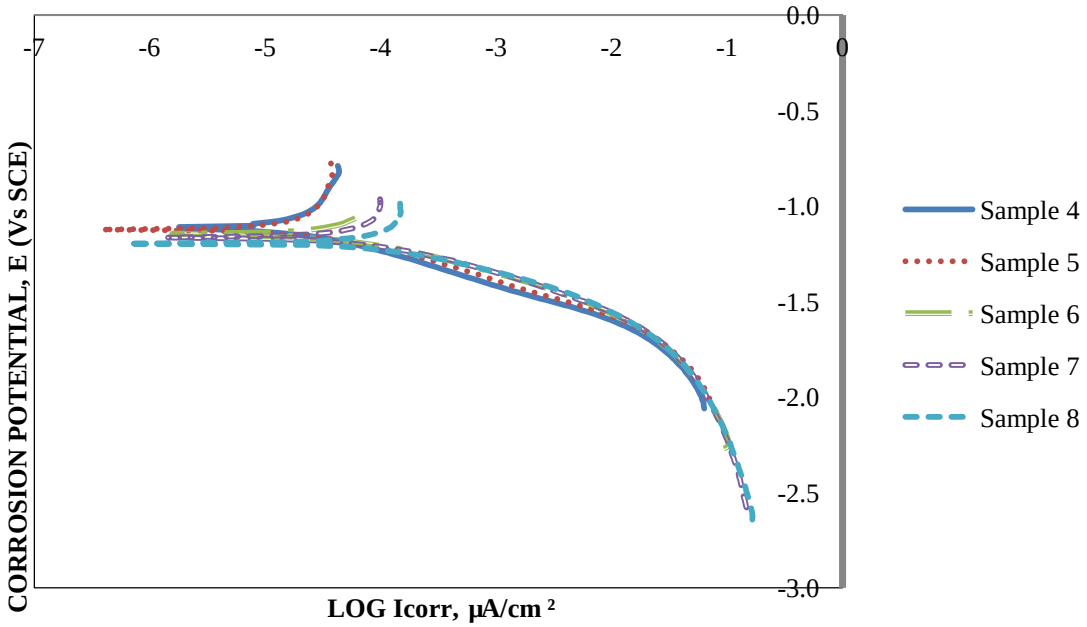

Figure 4.2: Polarization graph of different temperature solution

4.3 WEIGHT LOSS METHOD RESULTS

Based on Table 4.3, weight of samples for before and after natural corrosion had been recorded. The difference weight between them is calculated and the corrosion rate for each sample calculated by equation 2.6 in section 2.4.

The corrosion rate for sample 9 is 0.2517 mmpy. This values increases 36.4 % when the concentration of NaCl is 4.5%wt. The sample increased for 86.4 % became 0.4692 mmpy compare with sample 9.

Table 4.3: Data of samples of weight loss test

Sample	Weight (g)			CR	CR
	Before	After	Difference	(Mpy)	(mmpy)
9	6.426	6.404	0.022	9.926	0.2517
10	11.003	10.973	0.030	13.536	0.3433
11	9.472	9.431	0.041	18.499	0.4692

$$\boldsymbol{CR} = \frac{\boldsymbol{W\ x\ K}}{\boldsymbol{D\ x\ A\ x\ T}} \qquad \text{Equation 2.6}$$

CR – Corrosion rate, mm / year

K – 3.45 x 10^6 (for CR in MPY)

– 8.75 x 10^4 (for CR in mmPY)

W –weight loss in grams

D – Density in gram/cm ^{3}

A – Sample area in cm ^{2}

T – Exposed time in hours

Calculation example for sample 9 by using equation 2.6:

$$\boldsymbol{CR} = \frac{\boldsymbol{W\ x\ K}}{\boldsymbol{D\ x\ A\ x\ T}}$$

$$= \frac{\boldsymbol{0.022\ x\ (3.45\ x\ 10^6)}}{\boldsymbol{2.7\ x\ 2\ x\ (59\ x\ 24)}}$$

$$= \boldsymbol{9.926\ Mpy}$$

$$\boldsymbol{CR} = \frac{\boldsymbol{EW\ x\ K}}{\boldsymbol{D\ x\ A\ x\ T}}$$

$$= \frac{\boldsymbol{0.022\ x\ (8.75\ x\ 10^{46})}}{\boldsymbol{2.7\ x\ 2\ x\ (59\ x\ 24)}}$$

$$= \boldsymbol{0.4692\ mmpy}$$

4.4 EFFECT OF SOLUTION CONCENTRATION ON CORROSION RATE

Figure 4.3 shows the effect of Cl^- ions on the corrosion potential. These figure shows that the corrosion potential, E_{corr} shifts to more negative values as the Cl^- concentration increases at room temperature.

Efird et.al (1979) mentioned that the passivation reaction is independent of the Cl^- concentration and it is the breakdown passivity that is directly affected by Cl^- at certain temperature for AA6061-T6.

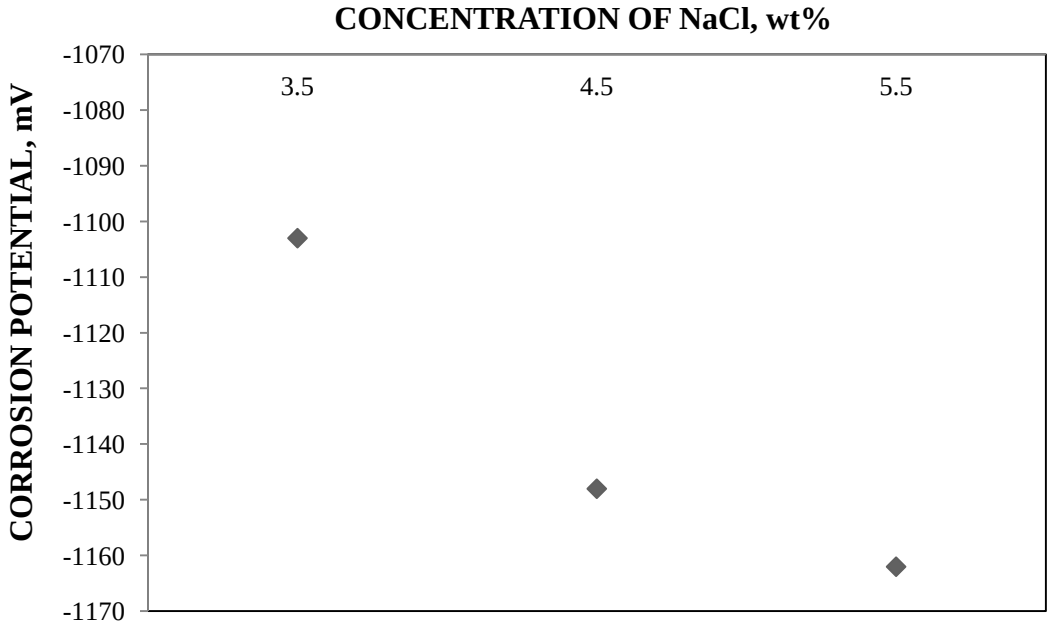

Figure 4.3: Effect of the concentration of NaCl solutions on the corrosion potential of AA6061-T6 at room temperature

Generally, the anodic process associated with the metal passivation is strongly affected by the presence of halide ions (NaCl) in the electrolyte. At the higher concentration of halide ions, the passive film susceptible to pitting suffers local damage, while higher concentration causes an increasing of the i_{corr}.

Figure 4.4 shows the relationship between the corrosion rates with the concentration of NaCl solution for AA6061- T6. It indicates that at constant temperature,

the corrosion rate increases as the concentration of Cl^- increases. Once a pit initiates, a passive – active cell is set up of large potential difference. The resultant high current density accompanies a high corrosion rate of anode and polarizes the surface immediately surrounding the pit to a value below the critical potential. Through flow of current Cl^- ions transfer into the pit forming concentrated solution of Al^{3+} chlorides, which by hydrolysis account for an acid solution. The high Cl^- concentration ensure that the pit surface remain active.

Moreover increasing the Cl^- leads to increase the conductivity of the solution and as a result the corrosion current density also will increase.

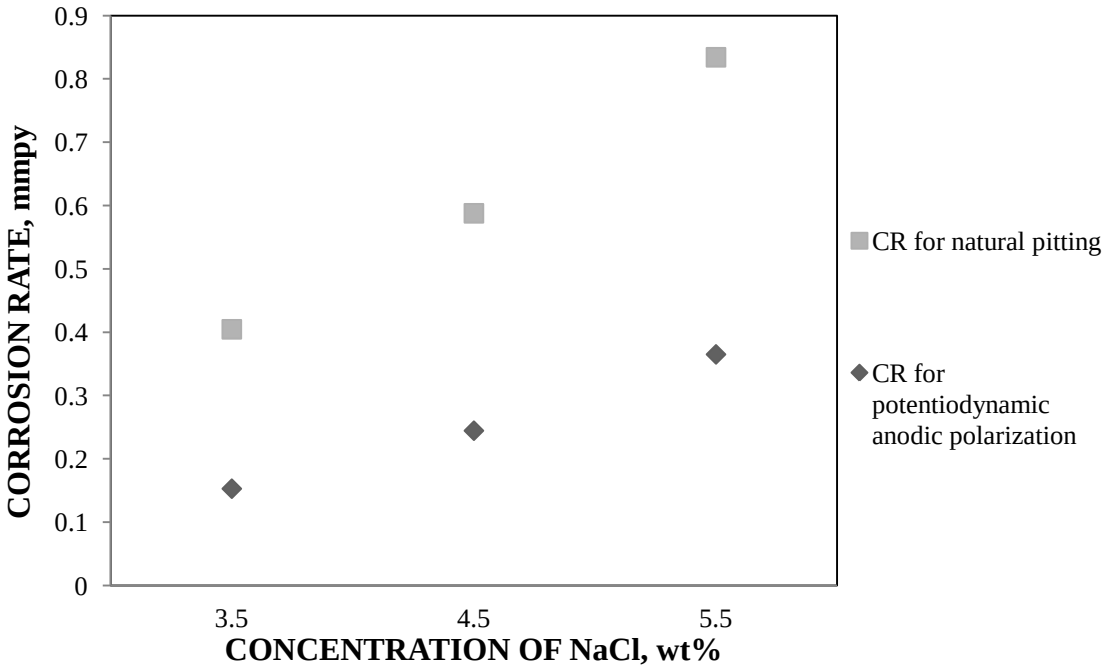

Figure 4.4: Comparison of corrosion rate between 2 methods

4.4.1 COMPARISION OF COROSION RATE BETWEEN ELECTROCHEMICAL TEST AND NATURAL PITTING TEST

Figure 4.5 shows that the natural pitting test result is higher than the electrochemical test. This is because there had many other environment effects act on natural pitting test. In the natural pitting test, the pipe water is use as solution. Many

water quality factors affect corrosion of metal used in water distribution, including the chemistry and characteristics of the water, salts and chemicals that are dissolved in the water, and the physical properties of the water. Waters differ in their resistance to changes in their chemistry. All waters contain divalent metals such as calcium and magnesium that cause water to have properties characterized as hardness and softness.

Alkalinity is a characteristic of water related to hardness. Waters with low hardness, or alkalinity (less than 50 mg/L as calcium carbonate), are more susceptible to the factors affecting corrosion. The alkalinity of pipe water is lower than distill water. Therefore, corrosion rate of natural pitting is higher than electrochemical test.

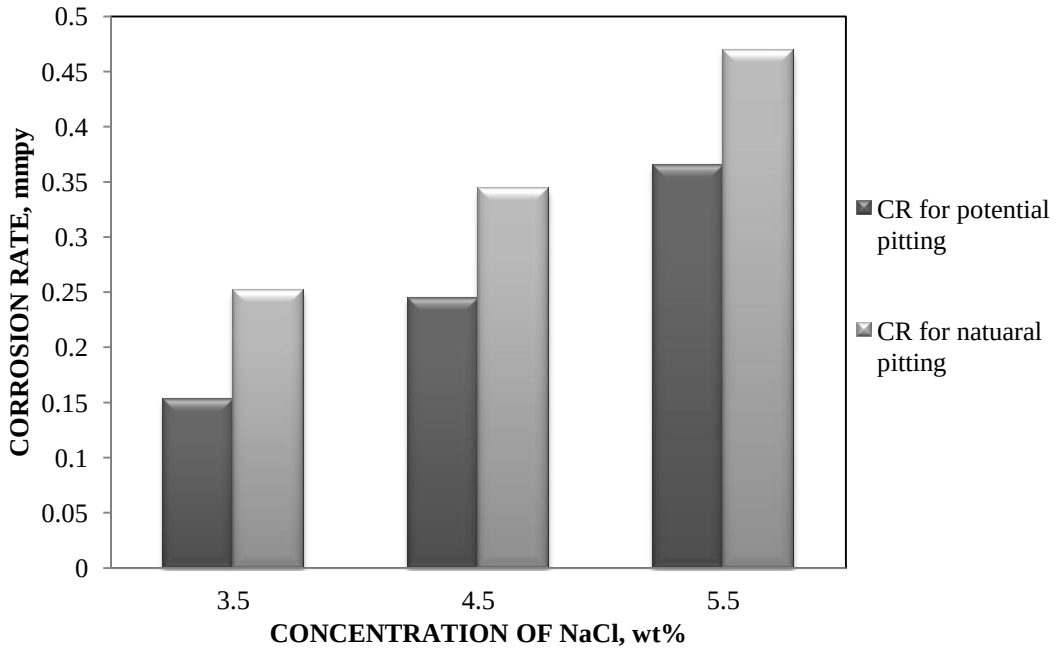

Figure 4.5: Comparison of corrosion rate between electrochemical test and natural pitting test

4.5 EFFECT OF TEMPERATURE ON CORROSION RATE

Figure 4.6 shows the effect and the relationship between the corrosion potential (E_{corr}) of AA6061-T6 aluminium alloy with different temperatures in concentrations 3.5 wt% of NaCl solutions. From Figure 4.6, it can be seen that as the temperature of the

solution increases the corosion potential decreases, i.e, shift of corrosion potential to more active direction, this indicates that the pitting resistance of AA6061-T6 decreases with increasing temperatures.

Most of the electrochemical reactions reacted more rapidly at higher temperature. Therefore the rate of pitting would increase as the temperature increases, as shown in Figure 4.7. Processes accompanying pitting are active dissolution of AA6061, growth of the oxide film, dissolution of the oxide film, diffusion of various species through the oxide film into and out of the pit and formation of salt layer on the bottom of the pit. Rate of the above reactions increases with temperature. So as the diffusion of chloride ion through the passive film increases, the pitting susceptibility of the alloy increases.

Similar results on the effect of temperatures to that of the present study was noticed by Leckie et.al (1996)**,** on austenitic 18:8 SS in 0.1M NaCl. They found that it had higher potential rate in $0^{o}C$ but this value decreased in $25^{o}C$. They attributed this high shift to the active direction when the temperature increases, due to the high chemical affinity of this SS for water at temperatures around room temperature. Therefore, it is difficult for Cl^{-} to displace both water and oxygen adsorbed causing this noble potential at this temperature (room temperature and below). At higher temperatures the ability of Cl^{-} to displace water and oxygen adsorbed becomes effective.

Table 4.3 shows the values of corrosion current densities at different temperatures. This table indicates that at constant concentration, the corrosion current density increases as the temperatures increases. Since corrosion rate is directly proportional with current density, therefore corrosion rate increases as the temperature increases.

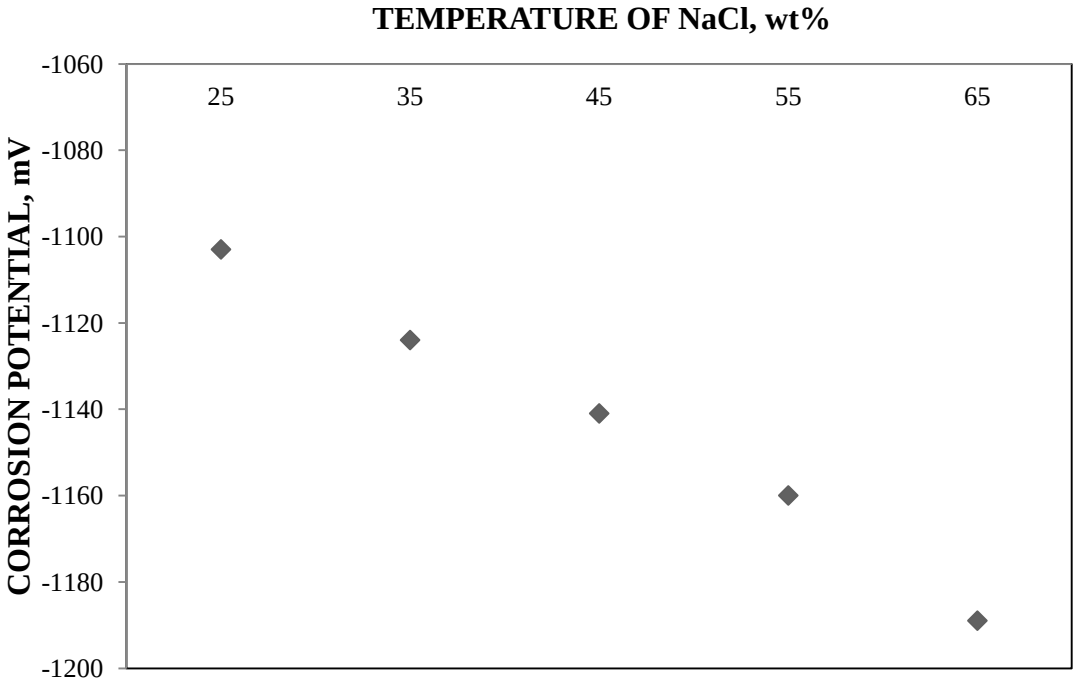

Figure 4.6: Corrosion potential versus temperature of solution

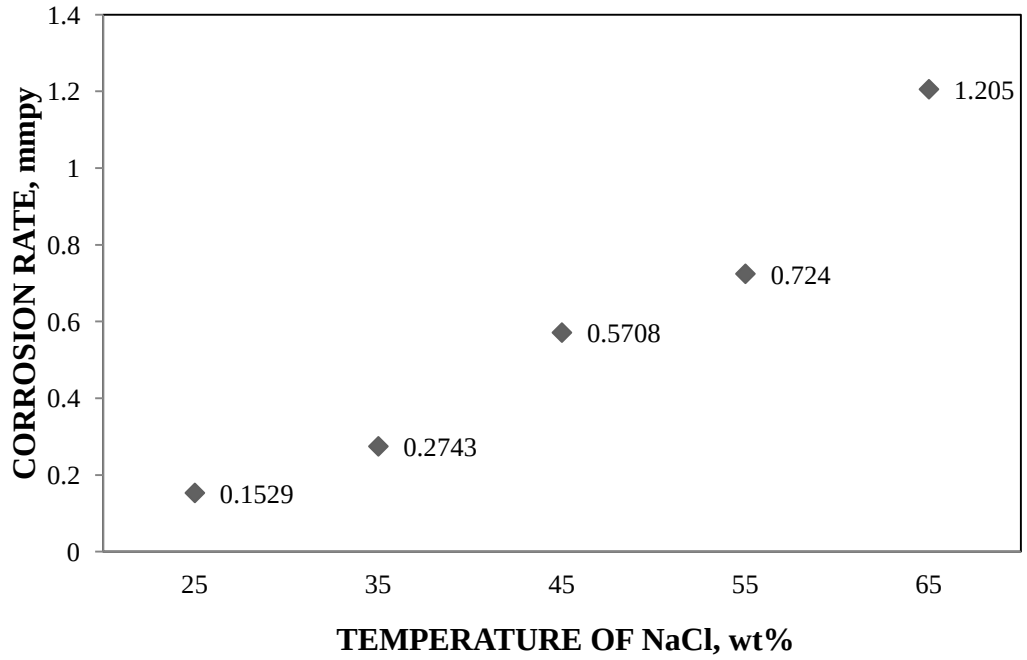

Figure 4.7: Corrosion rate versus temperature of solution

4.6 SCANNING ELECTRON MICROSCOPE (SEM) RESULTS

Figure 4.8 shows that all the microstructure of test sample by using the scanning electron microscope (SEM). The microstructure for sample 4 which tested in parameter of different temperature (25^{o}C) used the results of sample 1 because experiment condition of sample 4 was same with sample 1.

Based on the figures, type corrosion defect that formed in the experiment can be defined as pitting corrosion. In the SEM photo, the black hole or dark area showed as deep pit. Uniform pitting found at the surrounding of the deep pit. The pitting corrosion is promoted by the breaking-up of the protective oxide layer by a slip mechanism and the resolution of metal ions at the crack tip area. Cracks initiating from corrosion pits may grow by slip-oxidation mechanism.

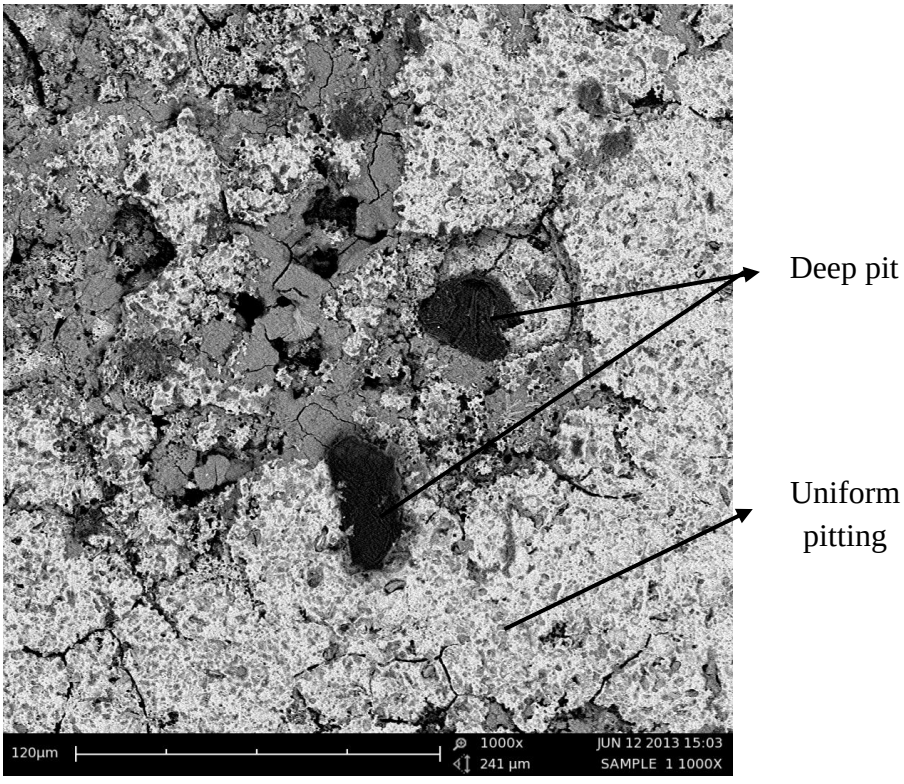

(a) Sample 1

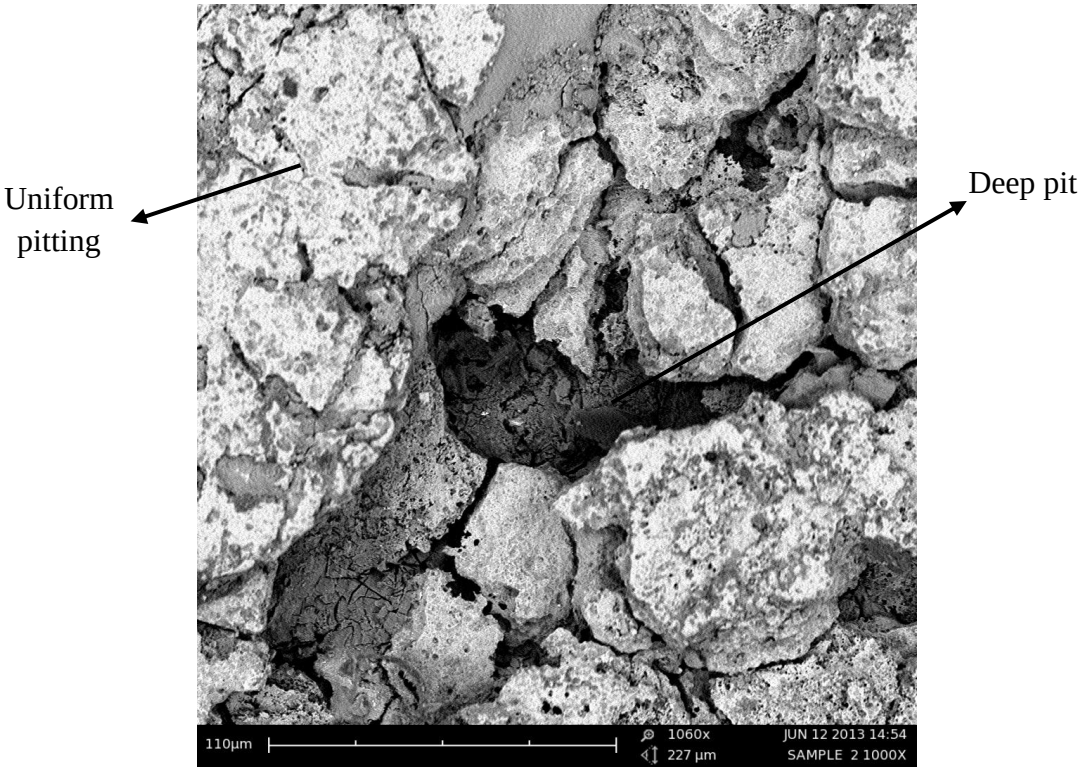

(b) Sample 2

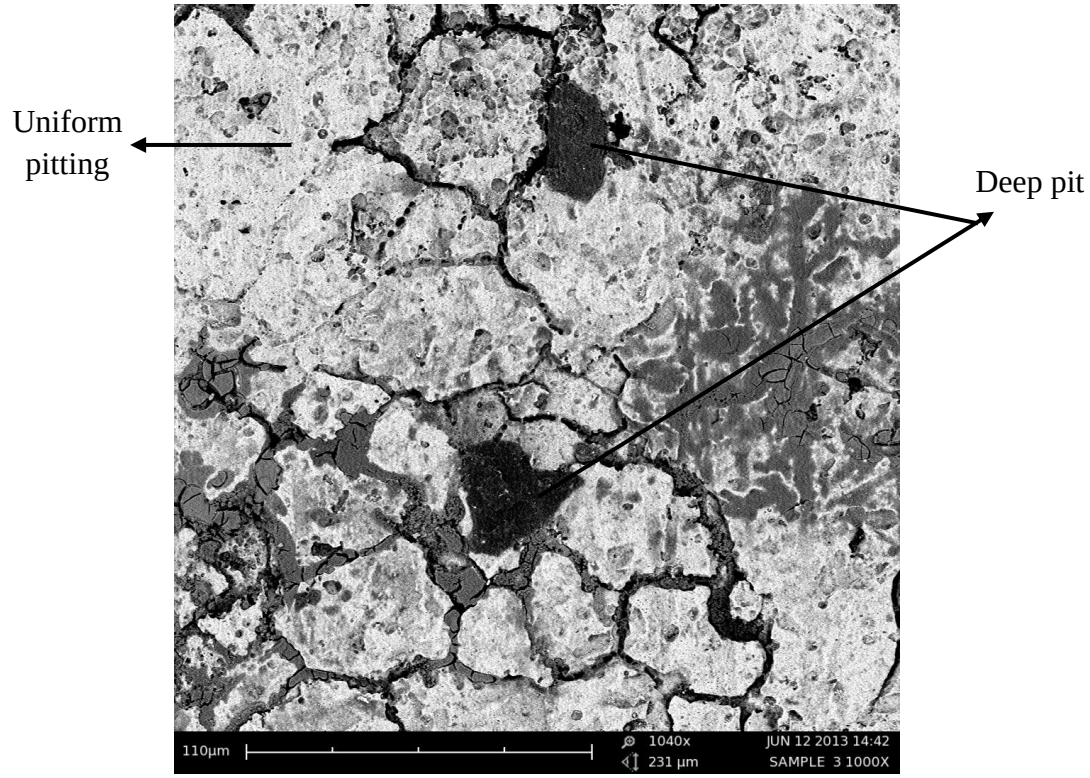

(c) Sample 3

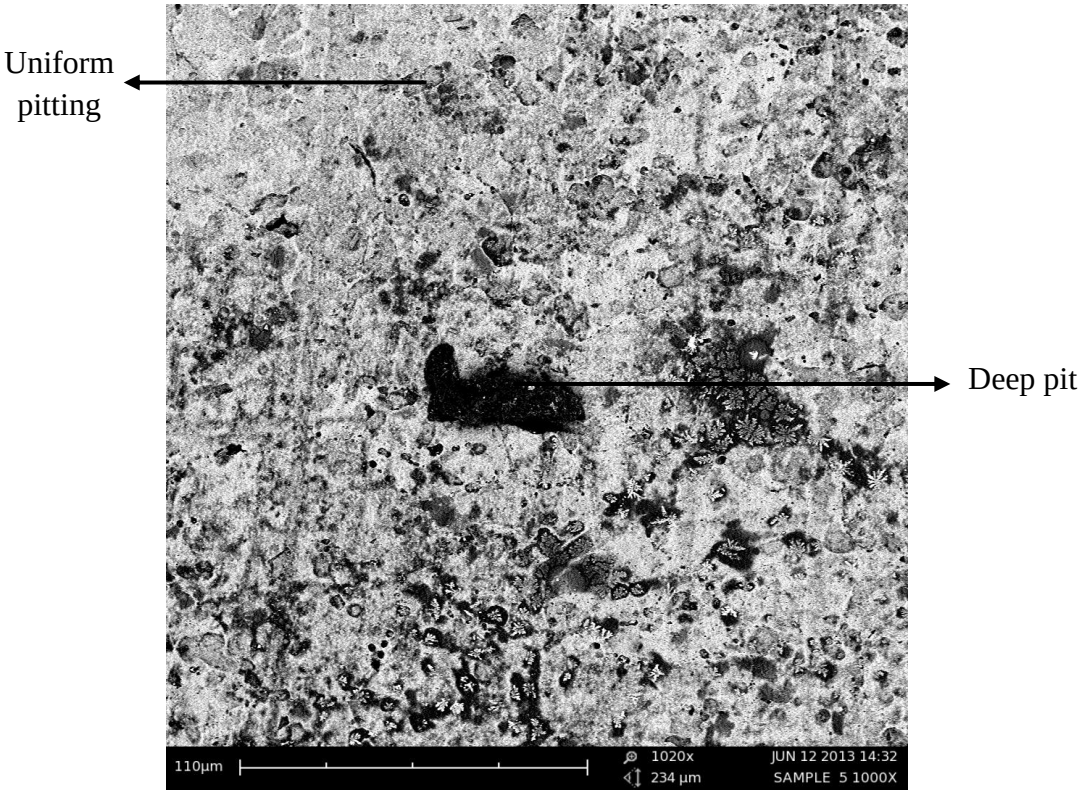

(d) Sample 5

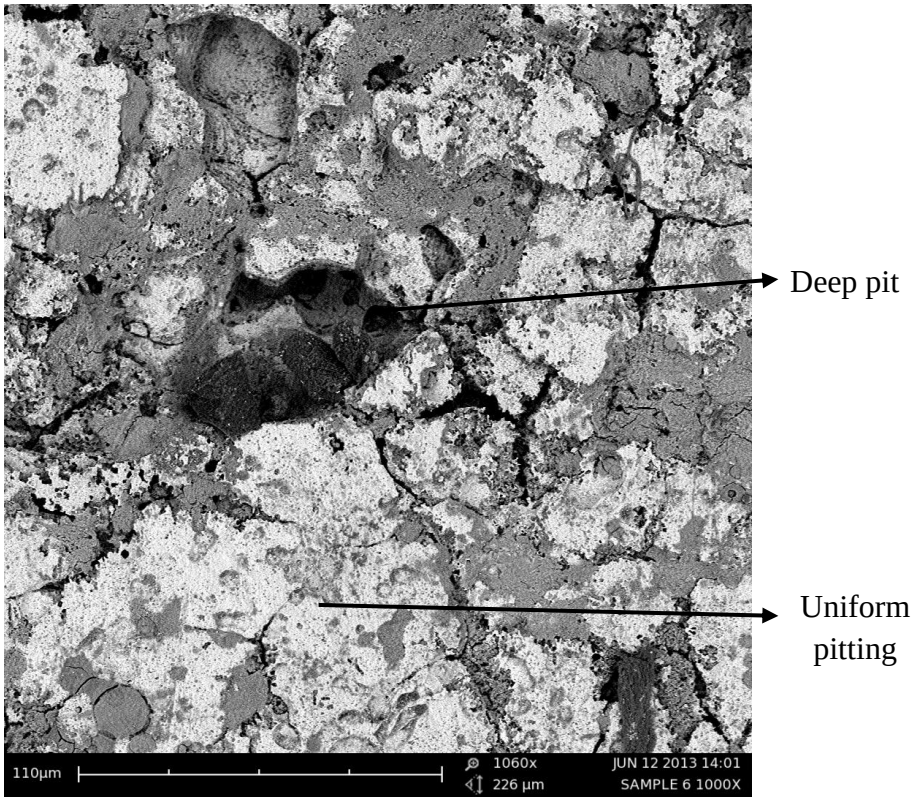

(e) Sample 6

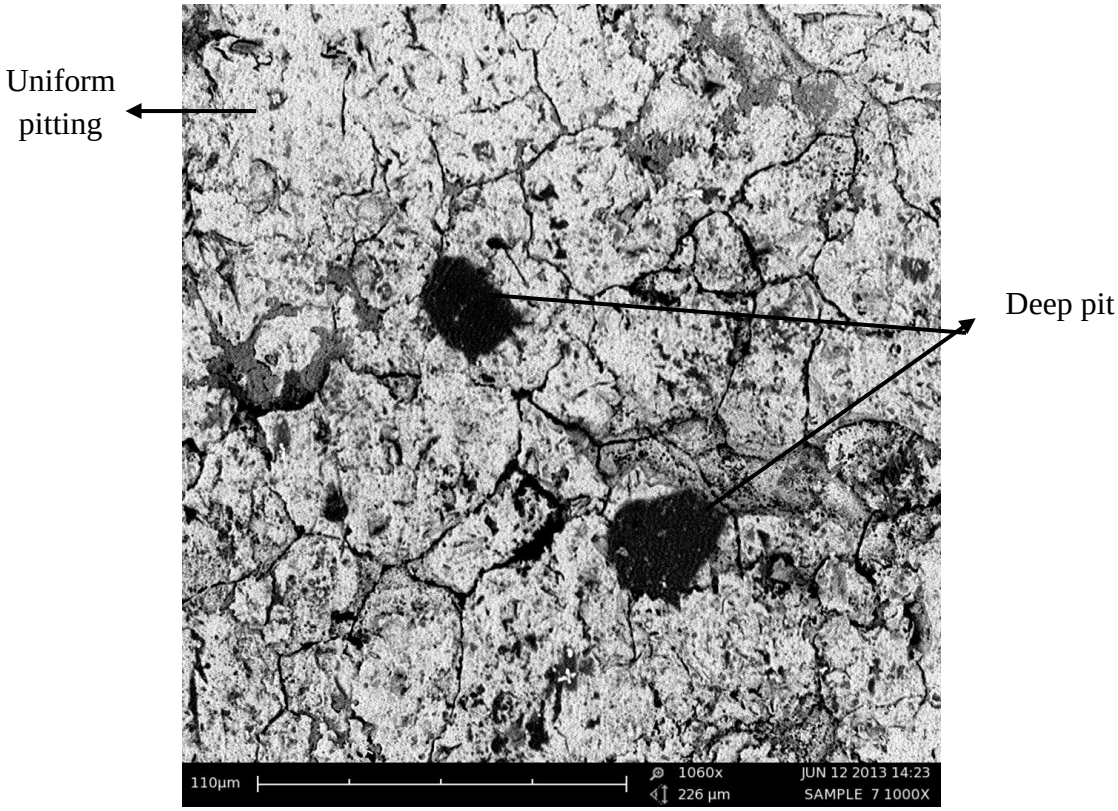

(f) Sample 7

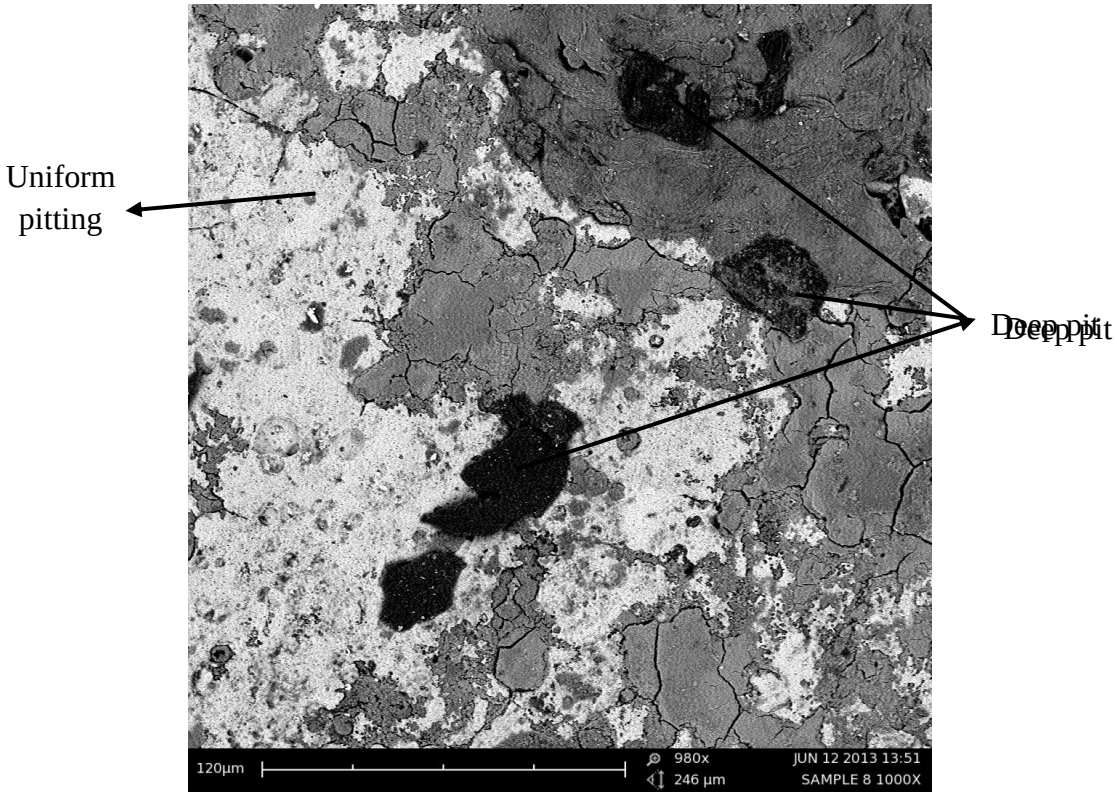

(g) Sample 8

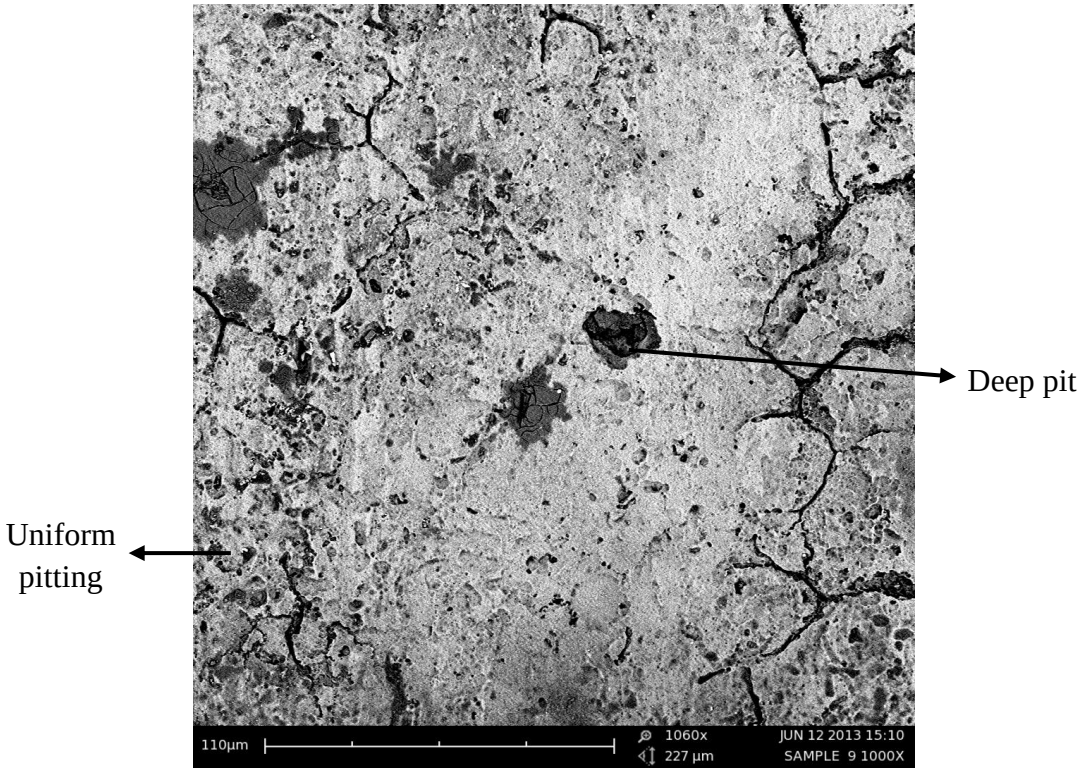

(h) Sample 9

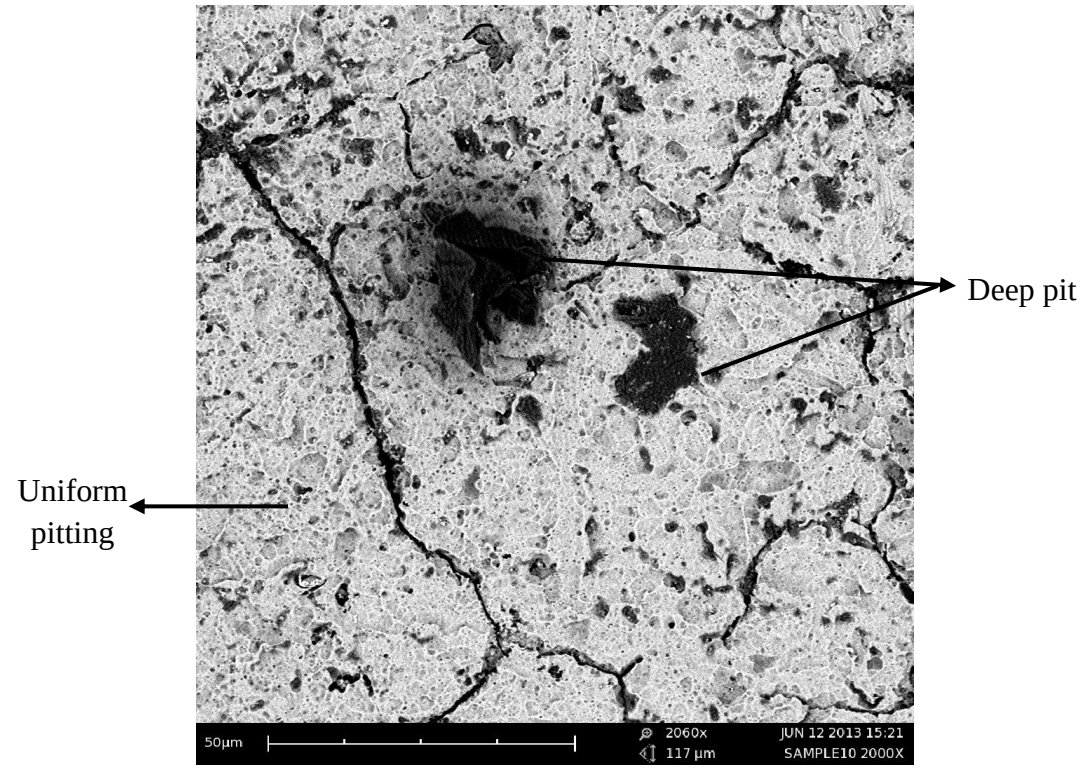

(i) Sample 10

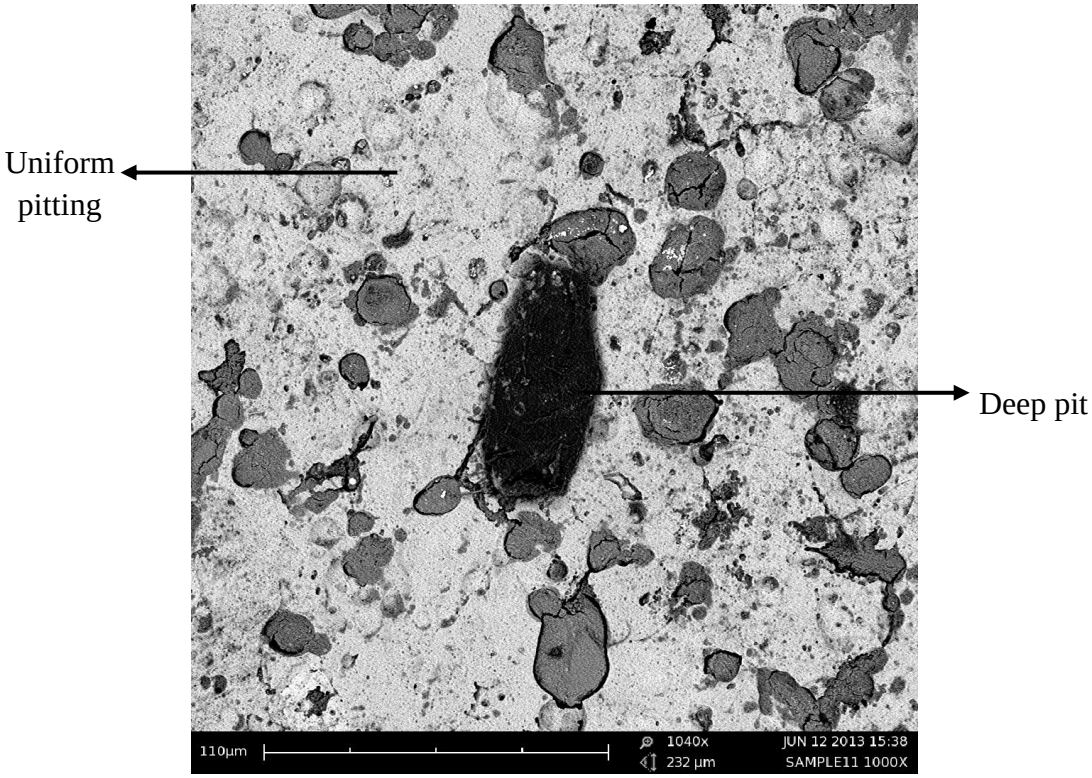

(j) Sample 11

Figure 4.8: Microstructure of each sample after experiment (1500x magnification)

CHAPTER 5

CONCLUSIONS AND RECOMMENDATIONS

5.1 INTRODUCTION

The corrosion rate of AA6061 aluminium alloy is tested in different concentration and temperature of NaCl solution. This project tested by two methods: weight loss method and potentiondynamic polarization. Due to previous chapter, a conclusion can be indicated. Therefore, the objectives of the study are proved.

Recommendation is provided in this chapter to investigate more about the pitting corrosion behaviour on aluminium alloys which can strengthen the research and provide new idea in corrosion science for the future study.

5.2 CONCLUSIONS

In the previous chapter, corrosion rate of sample increased when concentration and temperatures of NaCl solution increases. Therefore, the objective of this study is successfully obtained and fulfilled.

The sample that used in this study was analyzed by using spectrometer. The sample can be proved as AA6061 aluminium alloy by comparing its composition elements.

Sample 8 which tested in 65 ^{o}C in synthetic water has the highest corrosion rate which is 1.205 mmpy. The corrosion rate in different temperature is always increased when temperature of solution of NaCl increased.

Corrosion rate which tested in weight loss method and potentiodynamic polarization technique also increased when the concentration of chloride solution increased.

Therefore, this study can be concluded as corrosion rate of AA6061 aluminium alloy increases when temperature and concentration of solution chloride increases.

5.3 RECOMMENDATIONS

The effect of temperature and concentration of solution NaCl on pitting corrosion behaviour of aluminium alloy 6061-T6 are investigated in this study. However, there are many parameters can be test to enrich and increases the significant of the study. The recommendations should be considered for the future research study. Thus, for further work to study detail about this topic, some suggestions could be made into such as:

i. The effect of relative difference in velocity between the aqueous corrosive and the aluminium alloys' surface.
ii. The effect of alloy elements in the pitting corrosion resistance for other aluminium alloys.
iii. The influence of pH on the pitting corrosion behaviour on aluminium alloys under dynamic conditions can be studied.

REFERENCES

Alvarez. M.G. and Galvele J.R. 2010. Basic Concept, High Temperarue Corrosion. *Library of Congress Catalogue*. Number: 2009940135, ISBN: 978-0-444-52788-2. 4th edition. British: Elsevier Publications.

Ambat R. and Dwarakadasa E.S. 1993. Studies on the influence of chloride ion and pH on the electrochemical behaviour of aluminium alloys 8090 and 2014. *Journal of Applied Electrochemistry.* **24** (1994) 911-916

Avallone E.A., Baumeister III T. and Sadegh A. 2007. *Marks' Standard Handbook for Mechanical Engineers.* 11th ed. McGraw-Hill.

Cobden R. ,Alcan and Banbury. Aluminium. 1994. Physical Properties, Characteristics and Alloys. Training in Aluminium Applications Technologies.

Dimogerontakisa T., Campestrinib P. and Terryna H. 2006. The influence of the current density on the AC-graining morphology. *Electrochemical Society Proceeding*. **2004** (19) 402-405

Efird K.D. and George E.M. 1979. Material Performance, 18:9

Fontana M. G., Greene N. D. 1967. *Corrosion Engineering*. McGraw-Hill. (New York) **41**

Frankel .G.S., Stockert L., Hunkeler F., and Boehni H. 1987. *Corrosion.* **43**:429.

Frankel G. S. 1998. Pitting corrosion of metals a review of the critical factors. *Journal of the Electrochemical Society*. **145** (6): 2186-2198

Frankel G.S. 2006. Pitting corrosion. *Material Science and Engineering*. Fontana Corrosion Center, The Ohio State University

Günter S. 2009. Global needs for knowledge dissemination, research, and development in materials deterioration and corrosion control. *The World Corrosion Organization*.

Hewette D.M. 1978. Pitting of Austenitic Stainless Steel, the Electrochemical Basis and Validity of Potentionstatic Measuremens. master *Thesis, University of Tennessee Library* (Knoxville)

Jerzy B. and Igor S. 2007**.** *Corrosion Behaviour of and protection of copper and aluminium in seawater.* Feron D. (ed). **50** (1) 3-18.

Kalenda M. and Madeleine T. 2011. Corrosion fatigue behaviour of aluminium alloy 6061-T651 welded using fully automatic gas metal arc welding and ER5183 filler alloy. *International Journal of Fatigue*. **33**(12): 1539-1547.

Kaufman J. G. 2007.*Aluminium Alloys, in Handbook of Materials Selection.* Ed Kutz M. (New York) John Wiley & Sons, Inc.

Kemal N. Corrosion and protection of aluminium alloys in seawater. Norwegian University of Science and Technology

Key to Metal-The World's Most Comprehensive metals Database. n.d. Marine application of aluminium alloys: Part one (online). http://www.keytometals.com/Article99.htm (9 Octocber 2012)

Leckie H.P. and Uhlig H.H.1996. *Journal Electrochemical Society*, **113**:1262

Ma F.Y. 2012. Corrosive effects of chlorides on metals, Pitting Corrosion. Prof. Nasr Bensalah (Ed). ISBN: 978-953-51-0275-5. (China) InTech.

Majed R.A., Al-Kaisy H.A. and Al-Atrackchy H.B. 2008. Effect of chloride ions on the corrosion behavior of Al – Zn alloy in NaOH Solution at four different temperatures. *Al-Khwarizmi Engineering Journal*. **4** (4) : 26-36

Marine Applications of Aluminium Alloys: Part One. *Key to Metals.* The World 's Most Comprehensive Metals Database

Naseer A. and Khan A.Y. 2007 A study of growth and breakdown of passive film on copper surface by electrochemical impedance spectroscopy. *Tubitak Journal Chemical.*33 (2009), 739-750

Nik W.B.W., Sulaiman O., Fadhli A. and Rosliza R. 2010. Corrosion and protection of aluminium alloys in seawater. *The International Conference on Marine Technolog.*

One Steel –arrium Mining and materials. n.d. General Characteristics of Aluminium and Its Alloys (online). http://www.onesteel.com (19 November 2012)

Rao K.S. and Rao K.P. 2004. Pitting corrosion of heat-treatable aluminium alloys and welds: A review. *Transactions of the Indian Institute of Metal*. **57**:593-610.

Shaw B.A. and Kelly R. G. 2006. What is Corrosion? , *The Electrochemical Soiciety Interface.Spring*.

Shaw B.A., McCosby M.M., Abdullah A.M., and Pickering H.W. 2001. The Localized Corrosion of Al 6XXX Alloys. *JOM*. **53** (7): 42-46.

Skillingberg M. 2007. Aluminium at sea - Speed, endurance and affordability. *Marine Log.* 31 May.

Strehblow H.-H. 1976. Nucleation and Repassivation of Corrosion Pits for Pitting on Iron and Nickel, *Werk. Korros.* **27**:792

Strehblow H.H., Marcus.P. 1995. *Corrosion mechanism in theory and practice*. Series Corrosion technology (8). (New York) Dekker.M,

Szklarska-Smialowska Z. 1998. Pitting Corrosion of Aluminium. *Corrosion Science.* **41** (1999) 1743-1767.

Zhang L.H., Jiang Y.M., Deng B., Sun D.M., Gao J. and Li J. 2009. Effect of temperature change rate on the critical pitting temperature for duplex stainless steel. *Journal of Applied Electrochemistry*. **39**: 1703-1708

APPENDIX A1

COMPOSITIONAL ANALYSIS OF SAMPLE MATERIAL

Table A1: Compositional analysis of sample material

Element	Percentage (wt%)
Al	97.2
Si	0.825
Fe	0.416
Cu	0.217
Mn	0.109
Mg	0.794
Zn	0.0497
Cr	0.199
Ni	0.0132
Ti	0.0462
Be	< 0.0001
Ca	0.0071
Li	< 0.0001
Pb	0.0089
Sn	0.0301
Sr	< 0.0001
V	0.0107
Na	0.0109
Bi	0.069
Zr	0.0063
B	0.0021
Ga	0.0118
Cd	0.0012
Co	< 0.0030
Ag	< 0.0100
Hg	< 0.0030
In	< 0.0100

Source: Machine Spectrometer Foundry-MASTER FKM, UMP Pekan

APPENDIX A2

ALUMINUM ALLOYS: CHEMICAL COMPOSITION LIMITS

Table A2: Aluminium Alloys: Chemical Composition Limits

Elements in Percent, by Weight (maximum unless shown as range)

Alloy	Si	Fe	Cu	Mn	Mg	Cr	Zn	Ti	Other		Al
									Each	Total	Min.
1100	0.95 Si + Fe		.05-0.2	0.05	-	-	0.10	-	0.05	0.15	99.00
1145	0.55 Si + Fe		0.05	0.05	0.05	-		0.03	0.03		99.45
1200	1.00 Si + Fe		0.05	0.05	-	-	0.10	0.05	0.05	0.15	99.00
1230	0.70 Si + Fe		0.10	0.05	0.05	-	0.10	0.03			99.30
1235	0.65 Si + Fe		0.05	0.05	0.05	-	0.10	0.06			99.35
1350	0.10	0.40	0.05	0.01	-	0.01	0.05	-	0.03	0.10	99.50
2011	0.40	0.70	5.0-6.0	-	-	-	0.30	-	0.05	0.15	Bal.
2024	0.50	0.50	3.8-4.9	.3-.9	1.2-1.8	0.10	0.25	0.15	0.05	0.15	Bal.
3003	0.60	0.70	.05-0.2	1-1.5	-	-	0.10	-	0.05	0.15	Bal.
3004	0.30	0.70	0.25	1-1.5	8-1.3	-	0.25	-	0.05	0.15	Bal.
3005	0.60	0.70	0.30	1-1.5	0.2-0.6	0.10	0.25	0.10	0.05	0.15	Bal.
3015	0.60	0.70	0.30	.3-.8	0.2-0.8	0.20	0.40	0.10	0.05	0.15	Bal.
4047	11-13	0.80	0.30	0.15	0.10	-	0.20	-	0.05	0.15	Bal.
4045	9-11	0.80	0.30	0.05	0.05	-	0.10	0.20	0.05	0.15	Bal.
5052	0.25	0.40	0.10	0.10	2.2-2.8	.15-.35	0.10	-	0.05	0.15	Bal.
6061	0.4-0.8	0.70	.15-0.4	0.15	.8-1.2	.04-.35	0.25	0.15	0.05	0.15	Bal.
7072	0.07 Si + Fe		0.10	0.10	0.10	-	.8-1.3	-	0.05	0.15	Bal.
8011	50-0.9	0.6-1	0.10	0.20	0.05	0.05	0.10	0.06	0.05	0.15	Bal.
8111	30-1.1	0.4-1	0.10	0.10	0.05	0.05	0.10	0.06	0.05	0.15	Bal.

Alloys 1145,1230, 1235 - Vanadium 0.05 percent maximum

Alloy 2011 - Also contains 0.20-0.6 percent each of lead and bismuth
Alloys 1100, 4047, 4045 - Beryllium 0.0003 maximum for welding electrode and welding rod only

Source: The Oster Group (http://ajoster.com/)

APPENDIX A3

EQUIVALENT WEIGHT VALUES FOR VARIETY OF ALUMINIUM ALLOYS

Table A3: Equivalent Weight Values for a Variety of Aluminium Alloys

Common Designation	UNS	Elements w/Constant Valence	Variable Valence	Equivalent Weight
AA1100	A91100	Al/3	-	8.99
AA2024	A92024	Al/3, Mg/2	Cu/1	9.38
AA2219	A92219	Al/3	Cu/2	9.51
AA3003	A93003	Al/3	Mn/2	9.07
AA3004	A93004	Al/3, Mg/2	Mn/2	9.09
AA5005	A95005	Al/3, Mg/2	-	9.01
AA5050	A95050	Al/3, Mg/2	-	9.03
AA5052	A95052	Al/3, Mg/2	-	9.05
AA5083	A95083	Al/3, Mg/2	-	9.09
AA5086	A95086	Al/3, Mg/2	-	9.09
AA5154	A95154	Al/3, Mg/2	-	9.08
AA5454	A95454	Al/3, Mg/2	-	9.06
AA5456	A95456	Al/3, Mg/2	-	9.11
AA6061	A96061	Al/3, Mg/2	-	9.01
AA6070	A96070	Al/3, Mg/2, Si/4	-	8.98
AA6101	A96101	Al/3	-	8.99
AA7072	A97072	Al/3, Zn/2	-	9.06
AA7075	A97075	Al/3, Zn/2, Mg/2	Cu/1	9.58
AA7079	A97079	Al/3, Zn/2, Mg/2	-	9.37
AA7178	A97178	Al/3, Zn/2, Mg/2	Cu/1	9.71

Source: American Society for Testing and Materials (ASTM-G1)

APPENDIX B1

VISUAL INSPECTION OF DIFFERENT CONCETRATION FOR ELECTROCHEMICAL TEST

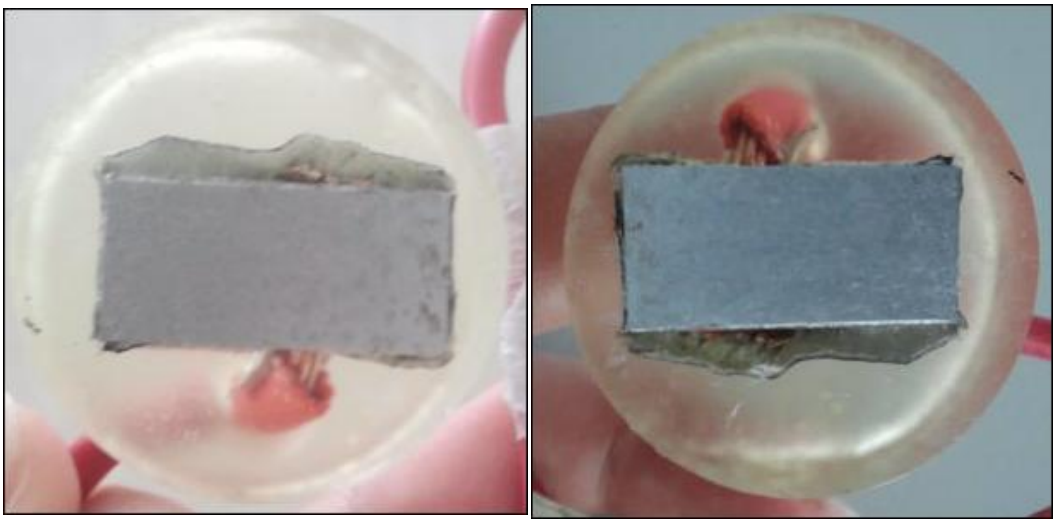

(a) Sample 1 (Before and after cleaning)

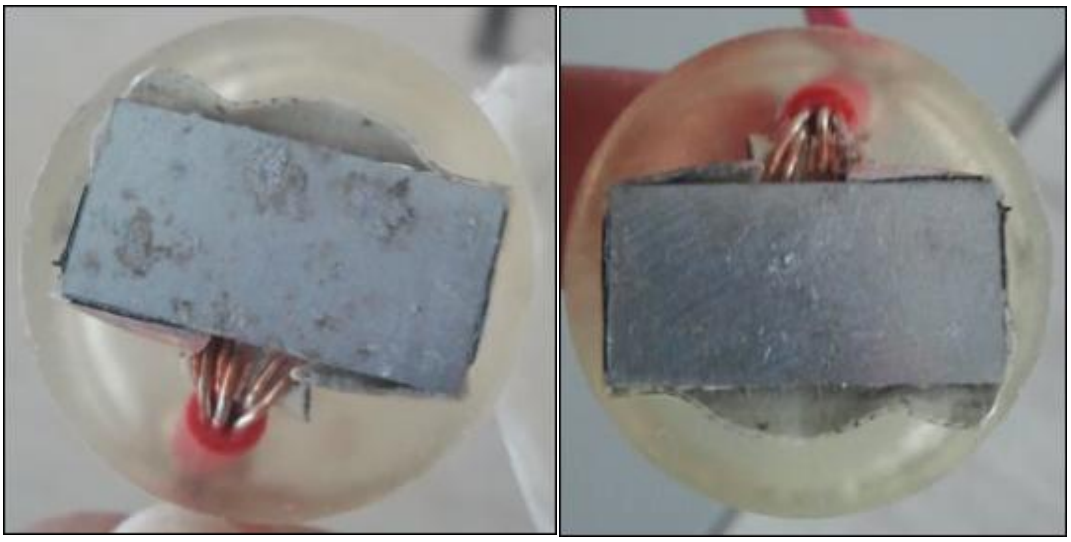

(b) Sample 2 (Before and after cleaning)

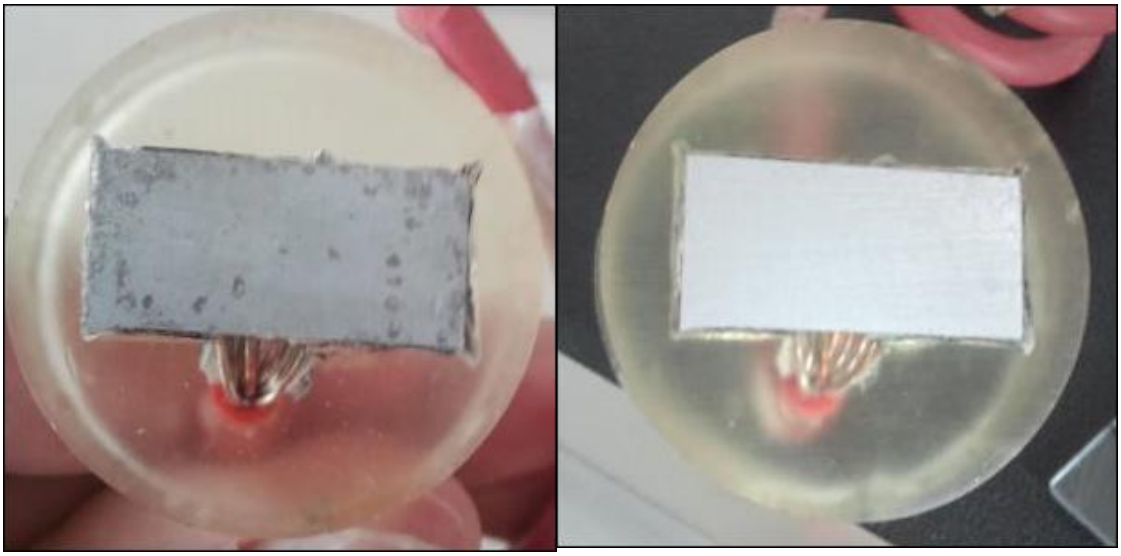

(c) Sample 3 (Before and after cleaning)

Figure B1: Visual inspection of test samples: (a) Sample 1, (b) Sample 2 and (c) Sample 3 before and after cleaning

APPENDIX B2

VISUAL INSPECTION OF DIFFERENT TEMPERATURE FOR ELECTROCHEMICAL TEST

(a) Sample 5 (Before and after cleaning)

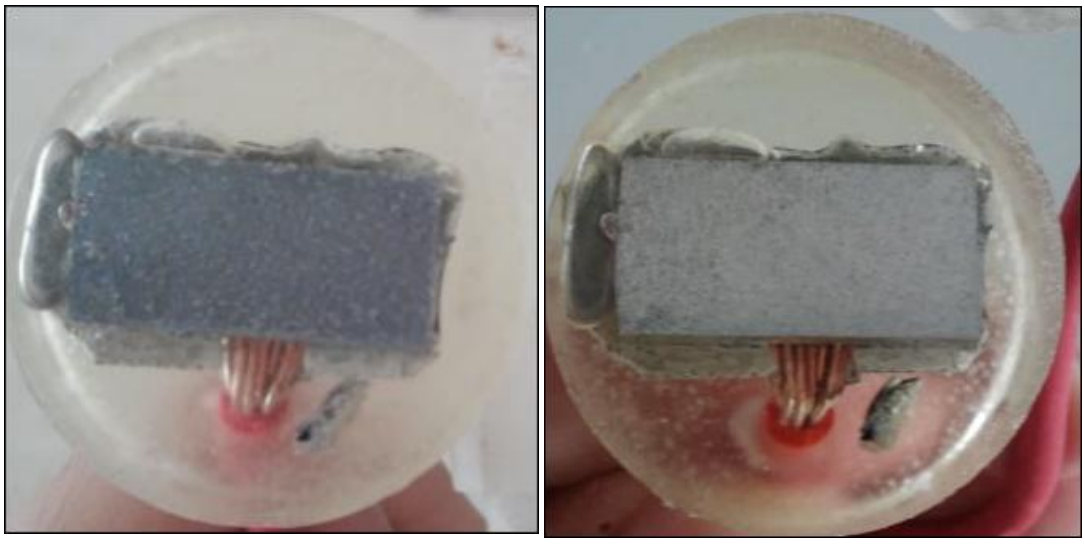

(b) Sample 6 (Before and after cleaning)

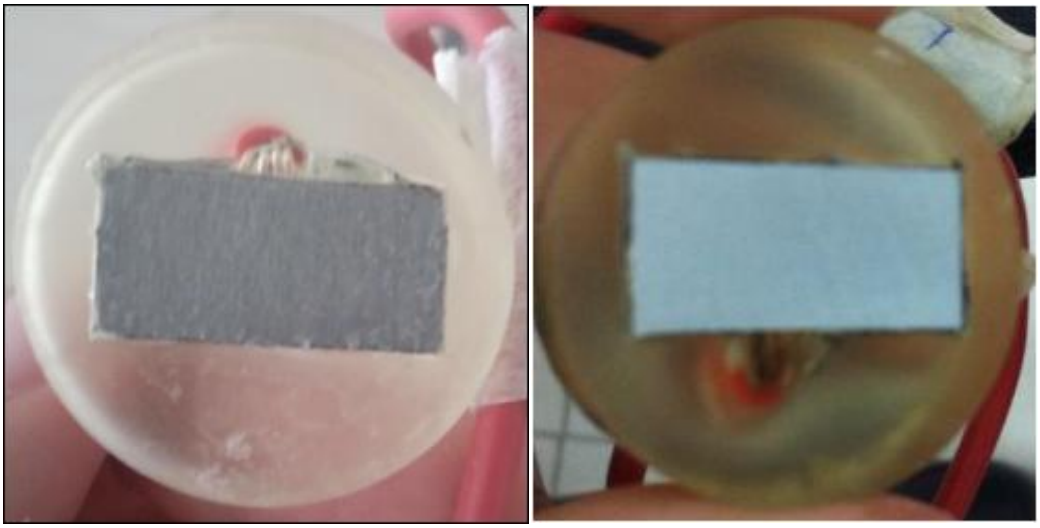

(c) Sample 7 (Before and after cleaning)

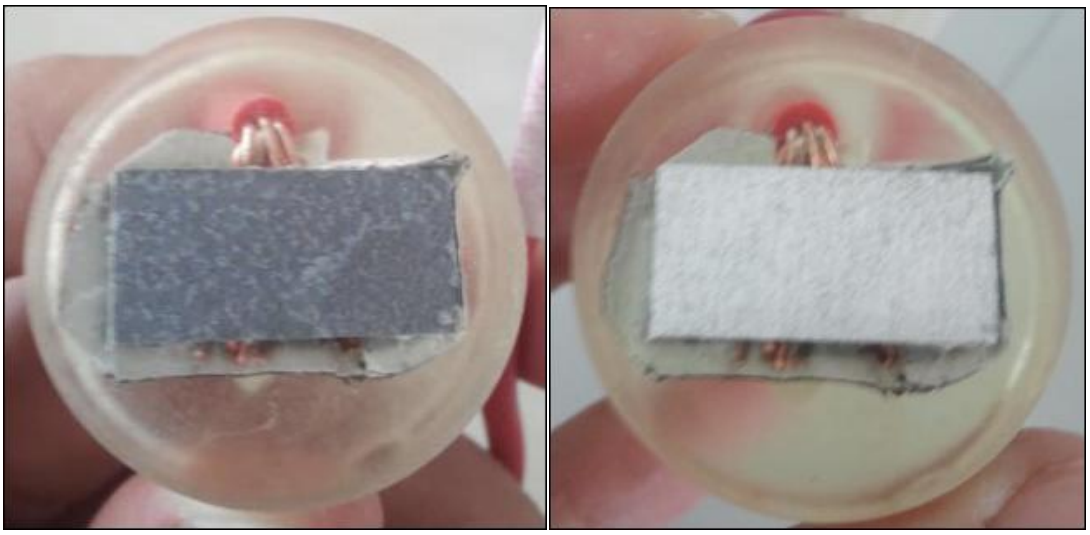

(d) Sample 8 (Before and after cleaning)

Figure B2: Visual inspection of test samples: (a) Sample 5, (b) Sample 6, (c) Sample 7 and (d) Sample 8 before and after cleaning

APPENDIX B3

VISUAL INSPECTION OF DIFFERENT CONCENTRATION FOR WEIGHT LOSS METHOD

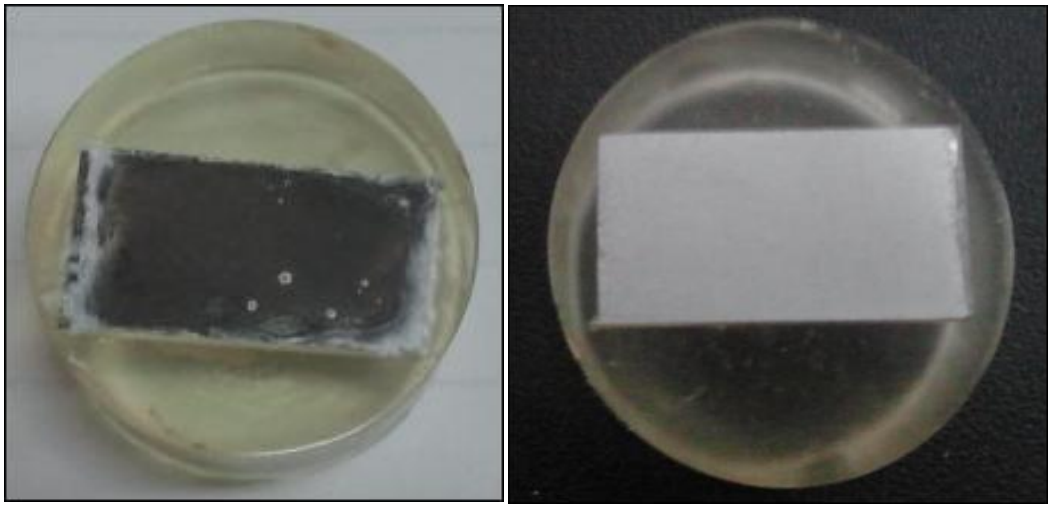

(a) Sample 9 (Before and after cleaning)

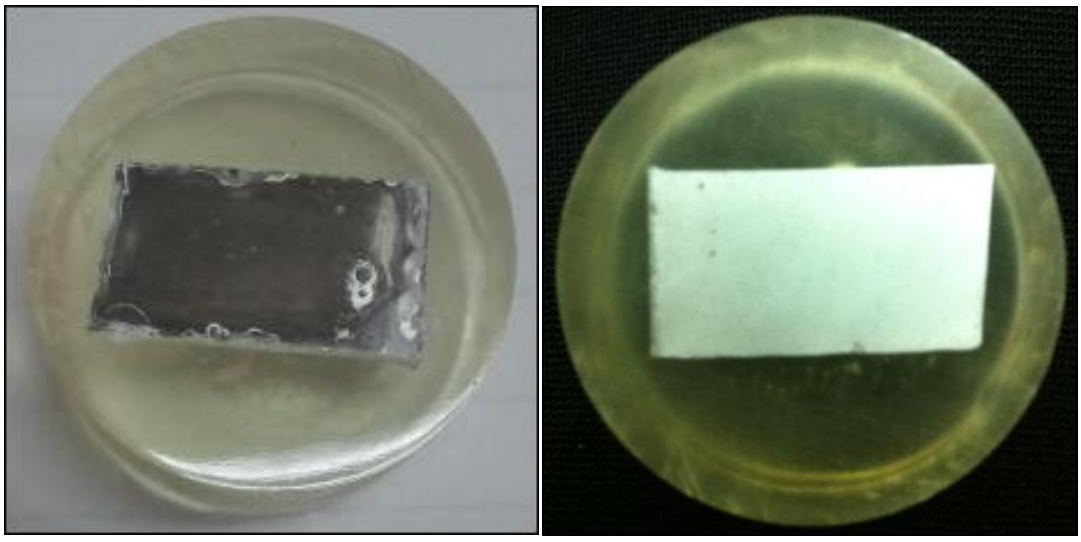

(b) Sample 10 (Before and after cleaning)

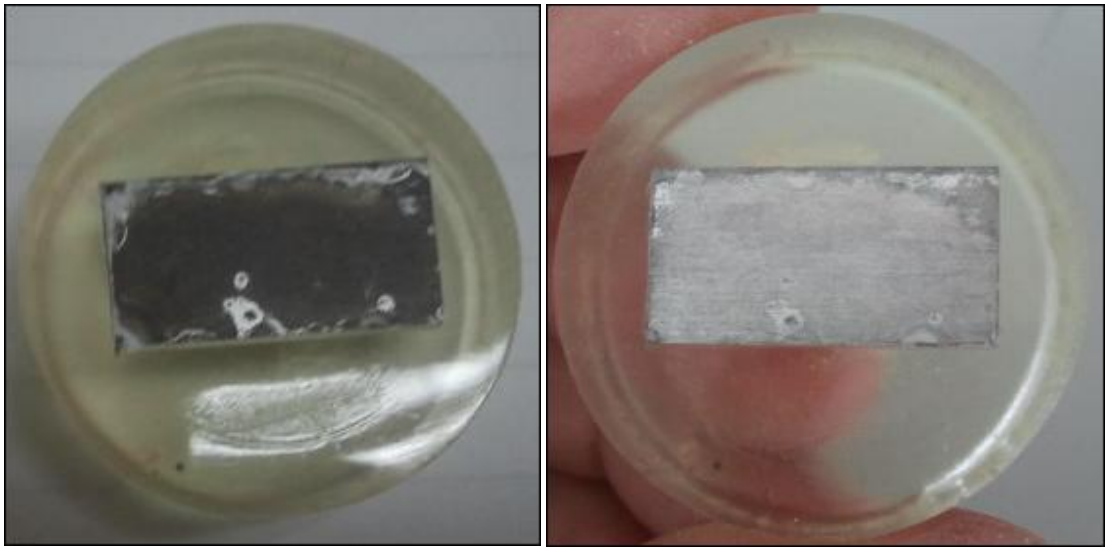

(c) Sample 11 (Before and after cleaning)

Figure B3: Visual inspection of test samples: (a) Sample 9, (b) Sample 10 and (c) Sample 11 after cleaning

APPENDIX C1

GANTT CHART PSM 1

TIME / PROJECT ACTIVITIES	Semester 1														
	Week 1	Week 2	Week 3	Week 4	Week 5	Week 6	Week 7	Week 8	Week 9	Week 10	Week 11	Week 12	Week 13	Week 14	Week 15
Discuss on the title of PSM 1															
Discuss on the objectives and the scopes															
Literature study and find the related info															
Discuss on the methodology and experiment set-up															
Finalize chapter 1, 2, and 3															
Report submission and presentation															

Planning Schedule	
Actual Schedule	

APPENDIX C2

GANTT CHART PSM 2

TIME / PROJECT ACTIVITIES	Semester 1														
	Week 1	Week 2	Week 3	Week 4	Week 5	Week 6	Week 7	Week 8	Week 9	Week 10	Week 11	Week 12	Week 13	Week 14	Week 15
Sample Preparation															
Microstructure Analysis															
Experiment Setup															
Electrochemical Test															
Result Analysis															
Report Writing															
Presentation															

Planning Schedule	
Actual Schedule	